2018

Nanofiltration of Perfluorinated Compounds as a Function of Water Matrix Properties

Hadi Toure
University of Central Florida

NANOFILTRATION OF PERFLUORINATED COMPOUNDS AS A FUNCTION OF WATER MATRIX PROPERTIES

by

HADI TOURE

B.S. University of Central Florida, 2016

A thesis submitted in partial fulfillment of the requirements
for the degree of Master of Science
in the Department of Civil, Environmental and Construction Engineering
in the College of Engineering and Computer Science
at the University of Central Florida
Orlando, Florida

Summer Term

2018

ABSTRACT

Perfluorinated compounds (PFCs) have been manufactured and used in various industries including food packaging, paintings, and coating industries. Perfluorooctanoic acid (PFOA) and perfluorooctane sulfonic acid (PFOS) are the most commonly investigated PFCs that have bioaccumulative properties and a strong persistence in environment. Despite the growing interest in using membrane technology to remove PFOA and PFOS from water, little information is available on the impact of natural water matrices on the removal of PFOA and PFOS when using nanofiltration (NF). The presence of natural organic matter (NOM) and cations (Ca^{2+} and Mg^{2+}) in water matrices and their interactions with the PFCs may significantly impact their removal efficiency. The current study compared the rejection of PFOA and PFOS from laboratory-prepared water (deionized water), surface water and groundwater using a commercial NF membrane (NE 70). Three different experiments were conducted for 20 hours using a bench- scale flat sheet unit. Feed and permeate samples were collected and analyzed to determine the PFOA and PFOS concentrations using liquid chromatography-tandem mass spectrometry (LC/MS-MS). The compound rejections varied from 71 to 80 % for PFOA and 42 to 80 % for PFOS. The results showed increased rejection of PFOA/S in the surface water and groundwaters when compared to the laboratory-prepared water. This is likely due to the presence of NOM and cations in the natural water matrices. The permeate flux declined (12.3-56.2 %) as more cations and NOM were present in the feedwater, suggesting that the increased rejection of PFOS in natural waters may be due to membrane pore blockage.

This thesis is dedicated to my parents and dear husband, thank you for your love and support.

ACKNOWLEDGMENTS

This work was possible thanks to the guidance and supervision of my faculty advisors Dr. A H M Anwar Sadmani and Dr. Steven J. Duranceau. My sincere appreciation goes to Dr. Woo Hyoung Lee for serving on my committee. I would also like to express my appreciation to the environmental engineering laboratory coordinator, Mrs. Maria Real-Robert for her assistance on the operation of the Liquid Chromatography Tandem Mass Spectrometry (LC/MS) instrument. The surface and groundwater samples used in the current study were provided by the UCF Drinking Water Research Group. Thanks to Carlyn Higgins for helping me in the laboratory, Daniel Whalen and Martin Coleman for assisting me in obtaining water quality parameters and Kunal Olimattel for his help with the flat sheet apparatus. Finally, my deepest gratitude goes to my family for following me in every step of this research, believing in me and providing the moral support to accomplish my goals.

TABLE OF CONTENT

LIST OF FIGURES

LIST OF TABLES

LIST OF ABBREVIATIONS

Da	Dalton
DFT	Density Functional Theory
DI	Deionized Water
DOC	Dissolved Organic Carbon
DOM	Dissolved Organic Matter
GAC	Granular Activated Carbon
HA	Humic Acid
ICP	Inductively Coupled Plasma
LC/MS	Liquid Chromatography/Mass Spectrometry
LFB	Laboratory Fortified Blank
LRB	Laboratory Reagent Blank
MDL	Method Detection Limit
mM	Millimolar
MW	Molecular Weight
MWCO	Molecular Weight Cutoff
NF	Nanofiltration

NOM	Natural Organic Matter
PFAA	Perfluoroalkyl Acid
PFAS	Perfluoroalkyls
PFC	Perfluorinated Compounds
PFCA	Perfluoroalkyl carboxylate
PFOA	Perfluorooctanoic Acid
PFOS	Perfluorooctane Sulfonate
PFSA	Perfluoroalkyl Sulfonate
RSD	Relative Standard Deviation
SDVB	Styrene Divinyl-Benzene
SPE	Solid Phase Extraction
SUVA	Specific Ultraviolet Absorbance
TDS	Total Dissolved Solids
TOC	Total Organic Carbon
USEPA	United States Environment Protection Agency
UV	Ultraviolet

CHAPTER 1. INTRODUCTION

Perfluoroalkyl substances (PFAS) are compounds that have been commercially produced in consumer products industries for many decades. These chemicals are commonly used for their foaming and coating properties in various applications (i.e. firefighting foams, food packaging, painting, cardboard coating, domestic non-stick cookware coating). Perfluoroalkyl acids (PFAA) are widely used PFAS consisting of a carbon-fluorine base structure linked to a functional group. PFAA may include a carbon-fluorine complex attached to a carboxylic acid group and a sulfonic acid group. Figure 1 illustrates the chemical classification diagram of PFOA and PFOS.

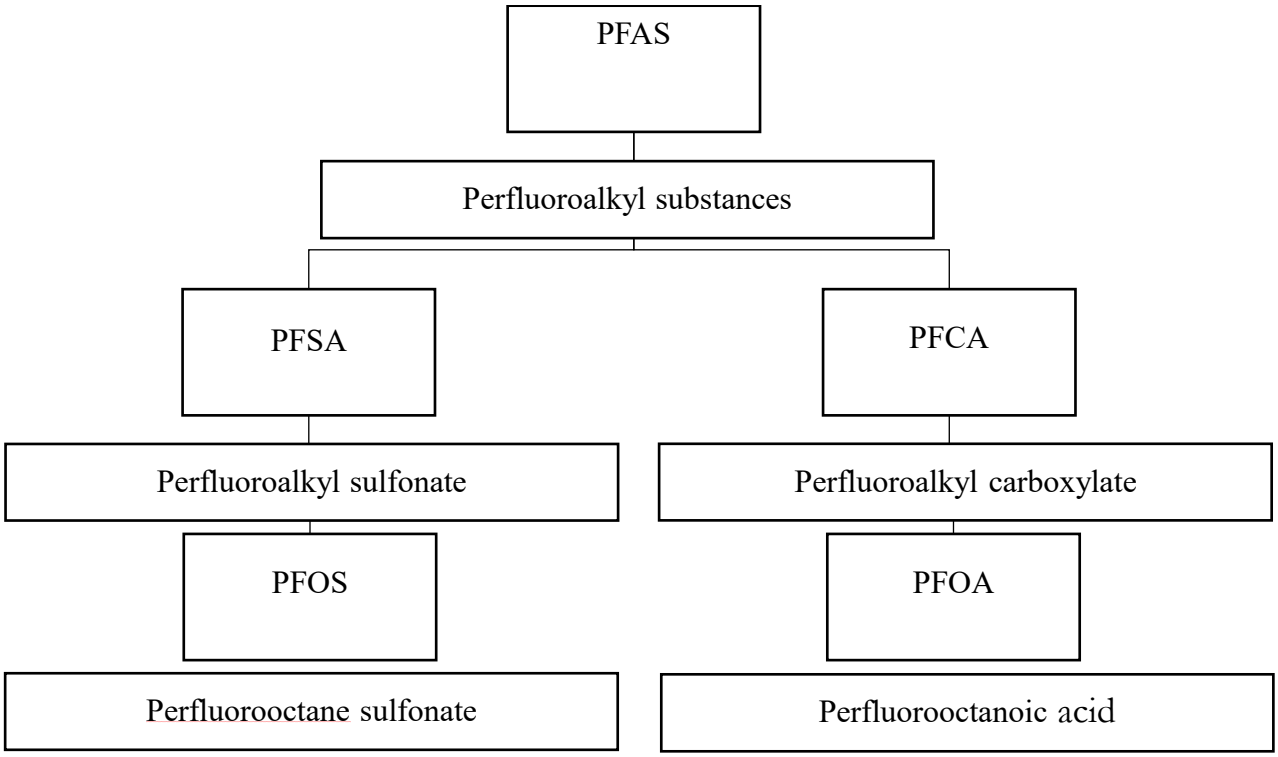

Figure 1: Chemical classification of PFOS and PFOA

The rigid polar covalent bond in the molecular structure of PFAS contributes to their persistence in the environment, which raised major environmental concerns. In fact, health issues including endocrine and neurological toxicity, and potential birth defects have been associated with mammal exposure to certain PFAS. The concern to limit human exposure to harmful dosages of PFAS has led to significant investigations and research. Despite the decline in production of common PFAS over the last decade, trace amounts are still present in drinking water, storm and wastewater, and biosolids in the United States. Particularly, the high solubility of (PFOA) and (PFOS) in water facilitates their pathway into natural water bodies, which makes their removal challenging using conventional water treatment methods.

Various existing water treatment techniques including granular activated carbon, ion exchange and membrane filtration have proven to be effective in removing most PFAAs from water. The detection of PFOA and PFOS in many surface and groundwaters across the United States justifies the growing interest in understanding the removal mechanisms and behavior of these compounds in different environments. Many researchers have contributed to provide a better understanding on removal techniques of PFAS from water, wastewater and soils. For example, removal methods include conventional treatments, adsorption processes (powdered and granular activated carbon), ion exchange, advanced oxidation and membrane treatment. Membrane separation is a physicochemical process involving the use of a semi-permeable synthetic membrane to separate impermeable molecules from water. Nanofiltration, often used to soften water and remove divalent ions, has been investigated as an efficient barrier to remove different PFAS from water. However, little information is available on the impact of natural water matrices on the removal of PFOA and

PFOS when using NF. This study investigated the influences of water matrices on the rejection of PFOS and PFOA when using NF. The specific objectives were:

1. To evaluate the rejection of PFOS and PFOA from various water matrices when using nanofiltration;
2. To determine the rejection of PFOS and PFOA as a function of water matrix properties.

CHAPTER 2. LITERATURE REVIEW

2.1 Emergence of PFOS and PFOA in Aquatic Environments

2.1.1 Toxicity of PFOA and PFOS

Since the 1950's, PFOS and PFOA have been commercially produced in the US in textile, packaging (fast food containers), painting, carpeting material, metal plating and aqueous firefighting foams industries. The complex structure of PFAS contributes to their industrial applications (Figures 2 and 3). Most PFAS include a hydrophobic fluorinated carbon chain, which facilitates their use in oil, soil and water resistant applications (Post et al., 2012). The proliferation and persistence in the environment of PFOS and PFOA is due to the carbon-fluorine bonds in their structure, which makes their decomposition and removal challenging. In fact, the hydrophobic fluorinated chain in common PFAS is usually linked to a hydrophilic carboxylic or sulfonic group that enhances high water-solubility. Additionally, PFOA and PFOS possess non-biodegradable, high polarity and stability characteristics. Over the last decade, PFOS and PFOA have risen environmental and health concerns due to their toxicity and bioaccumulation properties, leading to the discontinuity of the production of PFOS in the US in 2002 (Thompson et al., 2011). In contrast, PFOA and PFOA-related compounds that possess foaming and coating properties are still being produced by a limited number of industries. Nonetheless, concerns for the potential health effects of PFOA and PFOS have prompted the establishment of health advisory levels at 70 parts per trillion by the EPA (USEPA, 2016). In aquatic environments, rotifers, which are important species in freshwater and marine ecosystems, showed risks of population extinction under exposure to PFOA and PFOS (Zhang et al., 2014).

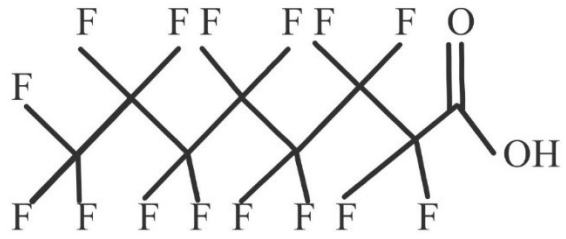

Figure 2: Chemical structure of perfluorooctanoic acid (PFOA)

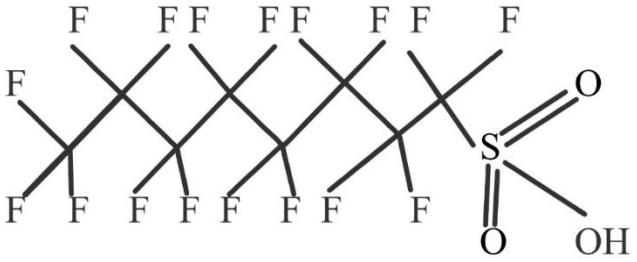

Figure 3: Chemical structure of perfluorooctane sulfonate (PFOS)

Beyond the potential toxic effects in aquatic ecosystems, both PFOS and PFOA have caused tumors in rats (Dickenson et al., 2016). Studies have shown that PFOA and PFOS persist in human serum with a half-life of up to 8.5 years and evidences in animal studies suggest high health risks to female and infants exposure (Post et al., 2012). In a recent study, both PFOA and PFOS had endocrine disruption effects in certain animal cells (Chaparro-Ortega et al., 2018). An in-vitro analysis of the human breast cells suggested that both PFAS have antagonist effects on sex steroid hormone receptors (Stigaard Kjeldsen et al., 2013).

2.1.2 Occurrence of PFOA and PFOS in Aquatic Environments

The main pathways resulting to the release of PFOA and PFOS to the aquatic environment include industrial discharge points as well as wastewater treatment plants and land application systems

(Suja et al., 2009). The release of the two compounds by industrial facilities can also occur through air pollution. This type of contamination is facilitated by wind transport and deposition of PFOA and PFOS particles on soils, rivers and potential migration in groundwater wells (Post et al., 2012).

PFOA and PFOS were documented in surface waters in several locations in the state of Georgia at concentrations up to 1,150 ng/L and 318 ng/L, respectively (Konwick et al., 2008). Furthermore, multiple drinking water and wastewater treatment plants across the United States contained PFOA and PFOS in their finished water (Quiñones et al., 2009). Similarly, significant concentrations have been found in groundwaters in the US including in Alabama, Michigan, New Jersey, Minnesota, Nevada, as well as in multiple cities in Western Europe (Xiao et al., 2015). Particularly, groundwaters contaminated by firefighting foams in New Jersey were identified with PFOA concentrations up to 190 ng/L (Post et al., 2009).

2.2 Removal Methods of PFOS and PFOA from Water

Various literatures have assessed removal techniques of perfluoroalkyl compounds from water. Prior investigations asserted that treatment processes including sand filtration, conventional treatment or oxidation were inefficient in removing perfluoroalkyl compounds when compared to membrane filtration, ion exchange and granular activated carbon (GAC) (Flores et al., 2013; Ochoa-Herrera et al., 2008)

2.2.1 Removal by Granulated Activated Carbon and Ion Exchange

Sorption by ion exchange or GAC has been characterized as economical ways to remove PFOS and PFOA from water. Adsorption of PFOS was investigated in exchange polymers (ion-exchange or non-ion exchange) and GAC in previous literatures (Senevirathna et al., 2010).

GAC is a treatment process involving the removal of dissolved particulates by adsorption into a porous carbon granule. In water treatment applications, GAC is used for dissolved organic compounds (DOC) and trace contaminants removal via a physical adsorption mechanism. Pramanik et al., (2017) has shown that GAC has a PFOS and PFOA removal efficiency of 80% and 78%, respectively. The study has also suggested that the presence of natural organic matter in the water matrix increases the removal efficiency of PFOS and PFOA by enhancing the reduction of sorption or pore sites on the GAC. Different sorption mechanisms were found to govern the removal of PFOS and PFOA including electrostatic, hydrophobic interaction and ion exchange (Q. Yu et al., 2009; Zaggia et al., 2016). Interestingly, contaminant breakthrough was a major inconvenience observed when using GAC as a removal technique for PFAS.

The use of strong anion exchange resins was considered as an alternative sorption method as compared to GAC due to regeneration limitations associated with activated carbon (Zaggia et al., 2016). Ion exchange mechanisms occur between an aqueous phase ion and a solid phase ion. An ion exchange resin is composed of exchangers with a fixed charged functional group combined with oppositely charged ions (or counterions) which interact with the bulk liquid phase (John C. Crittenden, 2012). Higher adsorption capacities were observed for PFOS and PFOA using anion-exchange resins as compared to commercial activated carbon. Such results were explained by the

presence of amine groups on the resin surface enhancing adsorption via anion-exchange (Du et al., 2015). Additionally, anion exchange resins demonstrated consistent results independent of the chain length of the compounds (Kothawala et al., 2017).

2.2.2 Removal by Nanofiltration

Membrane treatment processes involve the separation of water constituents using a semi-permeable synthetic membrane. Nanofiltration (NF) membranes are particularly used for water softening, brackish water and the removal of natural organic matter (NOM) to prevent disinfection-by-products formation. NF membranes are cost effective alternatives to reverse osmosis membranes for the removal of divalent ions and organic pollutants (John C. Crittenden, 2012). A number of studies have investigated the use of nanofiltration for removing organic micropollutants including pharmaceuticals (Sadmani et al., 2014). Similar research was performed to remove PFCs using nanofiltration. Also, a few researchers investigated the removal of PFOA and PFOS by nanofiltration using commercial membrane coupons (Hang et al., 2015; Pramanik et al., 2017; Soriano et al., 2017). Moreover, a rejection of 99% for PFOS and 97% of PFOA using laboratory scale testing with flat sheet membranes was documented by (Appleman et al., 2013). Dow Filmtech NF270 and NF90 membranes were particularly investigated in assessing the removal of perfluorinated compounds by nanofiltration. It was demonstrated that NF90 was more efficient in removing PFOS and PFOA from wastewater. PFOA showed a lower rejection (down to 92.2%) compared to PFOS due to its linear molecular shape (Hang et al., 2015). Previous work has shown the effective removal of PFOS in the presence of divalent cations (Mg^{2+}) using NF270 (Zhao et al., 2016). Such results suggested sieving as the governing mechanism in using nanofiltration to remove PFOS, due to the formation of magnesium and PFOS complexes. Research suggested

lower PFOS rejection in the presence of humic acid (HA) substances as opposed to Mg^{2+} (Zhao et al., 2016). In addition, Ca^{2+} ions enhanced the rejection of PFOS for similar reasons (Zhao et al., 2013). Although previous literatures tested different wastewaters and a few surface and groundwaters using nanofiltration, little research has been performed to compare PFOA and PFOS removal across different source water matrices. Table 1 summarizes the current findings on the removal of PFOA and PFOS by NF.

Table 1: Literature findings on PFOA and PFOS removal by NF

Compound	NF membrane	Water Source	MWCO	Conditions	Rejection	Authors
PFOA	NF90	Wastewater	90-200 Da	pH 6, T=25°C	99.3%	(Hang et al., 2015)
PFOA	NF270	Deionized water, Artificial Groundwater	200 Da	pH 6.7, T=18°C	97-99%	(Appleman et al., 2013)
PFOS						
PFOS	NF270	MilliQ water	200 Da	pH 4, T=25°C	90-99%	(Tang et al., 2007)
PFOS	HYDRACORE	Deionized water, Humic Acid solution	1000 Da	pH 7.5, T=20°C	40-60%	(Y. Yu et al., 2016)
	NF270		200 Da		>95%	

The effect of water constituents such as organic matter and cations were assessed by generating synthetic waters. The removal of PFOA by nanofiltration was assessed in groundwater and PFOA spiked deionized water (Boonya-atichart et al., 2016). No significant increase in rejection was observed with the groundwater as expected, but the authors showed a decrease in permeate flux due to high total dissolved solids (TDS) contents.

2.3 Factors Influencing the Removal of Organic Pollutants using Nanofiltration

The removal of trace organic compounds by nanofiltration is dependent on influencing factors affecting membrane-solute interactions. Parameters including membrane surface properties, compound molecular size and solute charge are important when evaluating rejection by NF.

2.3.1 Membrane Characterization Properties

Accurate measurements of membrane properties often facilitate the understanding of compound rejection. Membrane characterization yields important information correlated to the performance of the membrane for the removal of specific compounds. For instance, molecular weight cut-off (MWCO) is defined as the molecular weight at which 90% rejection is achieved. MWCO for commercialized NF membranes range from 300 to 500 Daltons (Da) (Labban et al., 2017). Although such measurements could presumably predict rejection of specific compounds of high molecular weights (MW), the MWCO is often a function of the organic pollutants used to achieve 90% rejection. Hence, MWCO should be used as a general guideline when comparing compounds with similar properties to those used to estimate the 90% rejection cut-off (Wilf, 2007). The desalting degree, defined as the percent rejection of a 500-2000 mg/L salt solution (usually sodium

chloride or magnesium sulfate), is also often considered as membrane characterization factor. Another factor influencing the rejection of organic pollutants is surface charge, commonly described by zeta potential measurements of the membrane. The surface charge on a membrane is usually dependent on the membrane's composition, specifically the functional group forming the membrane surface. As the feed conditions and pH varies, NF membranes can be either positively or negatively charged. For example, composite polyamide NF membranes can be negatively charged due to the carboxylate ion, COO^-, at the surface of the membrane resulting from the reaction between the membrane's aromatic ring and water molecules (Wilf, 2007). The principle that polymeric membrane surfaces can behave as amphoteric surfaces in neutral conditions (positively charged in lower pH range and negatively charged in higher pH ranges) was established in earlier literatures (Childress et al., 1996).

In addition, the membrane hydrophobicity/hydrophilicity is often estimated by its affinity with a water droplet on the membrane surface. The hydrophilicity of a membrane surface is experimentally represented by its contact angle with a water droplet. Contact angle measurements are influenced by electrostatic and hydrogen bond interactions between the membrane surface functional groups and the water molecules (Nicolini et al., 2016).

2.3.2 Solute Rejection Mechanisms

Although membrane surface properties determination provides general insights on membrane performance, thorough investigations on water matrix constituents and compound interactions is necessary to properly understand the underlying concept of membrane-solute interactions. NF membranes are subjected to complex selective rejection mechanisms categorized into three

distinctive components: steric interactions (Size exclusion), electrostatic effects (Donnan exclusion) and dielectric exclusion (Labban et al., 2017; Nicolini et al., 2016).

The rejection of organic compounds by NF is commonly attributed to the sieving or size exclusion effect. The mechanism of rejection based on the principle of sieving is a function of solute molecular size and geometry combined with the membrane pore size (Bellona et al., 2004). Despite the relevance of steric hindrance when evaluating the diffusion of solutes across a semi-permeable membrane, compound rejection should not be solely attributed to the sieving effect (Mohammad et al., 2002).

The electrostatic or Donnan exclusion effect is also a significant contributing factor to solute rejection across a membrane. Previous studies observed that for a negatively charged NF membrane, saline rejection was a result of anionic electrostatic repulsion and the attraction of divalent cations (Nicolini et al., 2016). However, as the cations concentration increased in the feed solution, a counter effect was observed due to the reduction of the electrical repulsion potential leading to the passage of anions across the membrane. This counter ion effect was hypothesized as the need to conserve electroneutrality across a membrane (Bellona et al., 2004). As cations bind to negatively charged functional groups at the membrane surface, higher cations rejection is observed. Additionally, the increase in ionic strength in the water matrix could lead to a gradual reduction of the membrane surface charge leading to a decline in PFA rejection (J. Wang et al., 2018). Overall, the removal of compounds by electrostatic charge repulsion may be strongly influenced by the water matrix components. Figure 4 depicts the two major rejection mechanisms investigated by previous literature.

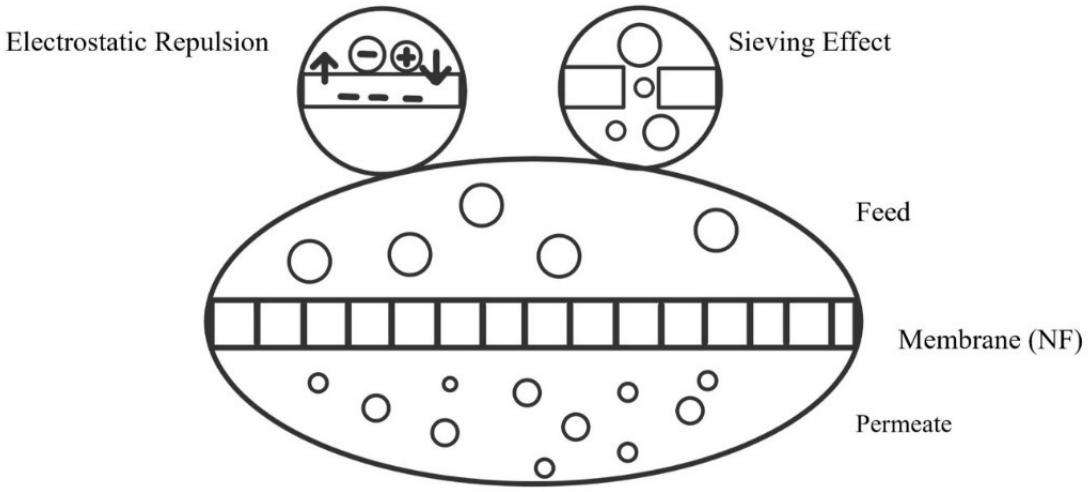

Figure 4: Major rejection mechanisms: sieving mechanism and electrical exclusion

The phenomenon of dielectric effect, classified by a few scholars as a non-steric rejection mechanism, is investigated by performing rejection experiments at the membrane isoelectric point, where the membrane surface charge is nullified at a specific pH (Childress et al., 1996; Nicolini et al., 2016). Dielectric exclusion conditions arise from the interaction of an ion with the interface between the membrane matrix and the bulk solution, consequently enhancing the accumulation of a distribution of polarization charge and a subsequent "image" ion (Oatley et al., 2012). Differences in dielectric constants between the membrane matrix and bulk solution result in repulsive forces between the ion and its "image" ion. The combined effects of both dielectric and steric interactions were observed in a study investigation the rejection of a range of 0.01 M salt solutions from two different membranes, as the isoelectric conditions across the membrane minimizes the possibility for Donnan interactions (Oatley et al., 2012). The results suggested higher rejection for sulfate (SO_4^{2-}) salts containing a divalent co-ion ($MgSO_4$ and Na_2SO_4) than

monovalent salts (NaCl and KCl). When comparing monovalent salts, rejection was higher for KCl containing K^+ ions, which are smaller than Na^+ ions. It was hypothesized that steric effects were less significant than dielectric effects.

2.4 Rejection of Perfluorinated Compounds as a Function of Water Matrix Components

2.4.1 Impact of Fouling on Rejection of PFOS and PFOA by Nanofiltration

Few investigations have been performed regarding the influence of fouling on the rejection of PFA substances. For example, Steinle-Darling et al., (2008) emphasized that membrane fouling decreased rejection of fluorinated compounds in deionized water. Thus, after a set of experiments on membranes (fouling simulations with alginate and chloride salts), the decline in rejection was explained by the occurrence of enhanced concentration polarization (accumulation of contaminants on the surface of the membrane). The efforts of Steinle-Darling et al., (2008) showed that although size exclusion remains the governing mechanism in particle rejection, the deposit of particles on the membrane surface could increase the chemical gradient, hence increasing the transport of particles in the permeate.

In contrast, membrane fouling did not decrease the rejection of PFOA and PFOS in other findings (Appleman et al., 2013). No significant decline or increase were observed with fouled membrane specimens with a solution of humic acid. Such results led to the argument that previous literatures (Steinle-Darling et al., 2008) did not adjust the membrane flux between virgin and fouled membranes. Thus, a significantly lower flux for the fouled membrane yielded lower rejection. Similar findings also indicated that properties such as water solubility and electrostatic charge

repulsion between PFOA and nanofiltration membranes dismissed membrane fouling issues (Hang et al., 2015).

Nonetheless, the fouling layer caused an increase in rejection of some PFAS (Appleman et al., 2013). These findings implied that enhanced compound rejection can occur due to the deposit of organic matter on the membrane surface, resulting in a change in membrane surface characteristics. In addition, the increase in rejection could also be due to solute-foulant interactions (Bellona et al., 2010; Yangali-Quintanilla et al., 2009). Thorough investigations on the impact of fouling behavior on the rejection of PFAS showed that although decreased rejection may be observed due to the weakening of electrostatic repulsion for smaller PFA molecules, increased rejection is generally observed with the presence of a fouling layer on the membrane surface (J. Wang et al., 2018).

2.4.2 Influence of Cations on the Rejection of PFAS

Although fewer researchers have explored the interactions between cations and PFOA (F. Wang et al., 2011), many publications have extensively studied the correlation between cations and PFOS rejection by nanofiltration. (Zhao et al., 2016) found that the presence of Mg^{2+} increased the rejection of PFOS whereas minimal improvement was observed in presence of humic substances. Similarly, an increase in PFOS rejection was observed by a hollow fiber NF membrane from 97.1 to 99.4% when calcium ions concentration increased in the solution from 0.1 mM to 2 mM (T. Wang et al., 2015). The same observations were observed from surface water containing calcium ions (Zhao et al., 2013). In a recent study, the main PFOS removal mechanism in the presence of cations was the sieving effect (Zhao et al., 2018). Most of the aforementioned studies demonstrated the evidence of a bridging effect between cations and PFOS molecules by density functional theory

calculation. It was further demonstrated that the binding effect between PFOS molecules and cation is a function of valence: divalent ions have the tendency to attract two PFOS molecules whereas monovalent cations such as Na^+ attract single PFOS molecules (Zhao et al., 2018). Analysis on the geometry of PFOS molecules suggested that the sulfonate group on the PFOS molecules reacts as a bonding site with positively charged calcium ions. Hence, the enhanced PFOS rejection was attributed to the complexation of larger PFOS-calcium molecules, leading to improved sieving effect.

CHAPTER 3. MATERIALS AND METHODS

3.1 Water Matrices Characteristics

An analysis of different background matrices was performed to study the impact of water matrix components on the rejection of PFOS and PFOA.

Table 2: Water matrix characteristics

Parameters	Deionized Water	Ocmulgee River	Jupiter Groundwater
pH	6.5	7.13	6.96
Temperature (°C)	25±0.5	25±0.5	25±0.5
Alkalinity (mg/L as $CaCO_3$)	Not Determined	34.5	300
Turbidity (NTU)		3	0.187
Conductivity (µS/cm)		126	801
TDS (mg/L)		64	555
Magnesium (mg/L)	0.06	2	5
Calcium (mg/L)	0.1	8	122
DOC (mg/L)	< 0.250	2.8	10.5
SUVA254 (L/mg-M)	0	0.09	3.93

The water sources analyzed in this study included three different matrices. Laboratory deionized water (DI) was used as a control experiment. The selected raw waters were collected in plastic containers and stored in a 4°C walk-in cooler until analysis. The samples characteristics were obtained within 14 days of collection date. Water matrix parameters for the control water and raw waters are summarized in Table 2.

The surface and groundwater samples selected for this study had distinctive properties. The surface water, collected in the Ocmulgee river (Georgia), showed significant turbidity and DOC concentration. The raw groundwater (Jupiter, Florida) contained significant TDS, conductivity and DOC. This water also indicated a calcium content of 122 mg/L compared to 8 mg/L for the surface water. The three waters were also screened for background PFOA and PFOS concentration. Each water was extracted using the protocol in section 3.5.1 and analyzed using the LC/MS instrument. For the DI, river and groundwater selected, PFOA and PFOS concentrations were below the detection limit of the LC/MS.

3.2 Selected Compounds Properties and Characteristics

PFOA (Sigma Aldrich, Saint Louis, MO, USA) and PFOS salt (Dr Ehrenstorfer GmbH, Augsburg, Germany) of purities 96 and 98.5% respectively were used to prepare stock standard solutions. The physicochemical properties of the PFOA and PFOS solutions are found in Table 3. These compounds were selected for this study as they represent significant concerns for drinking water treatment plants across the United States. PFOA and PFOS are the common PFAS found in drinking and wastewater (Thompson et al., 2011) and constitute a considerable threat to human health. PFOA and PFOS are known for their persistence in aquatic environments due to their

physical and chemical characteristics including chemical stability, low volatility and high water solubility (Xiao et al., 2012). PFOA and PFOS were detected by the LC/MS based on USEPA's method 537 (USEPA, 2016). Polypropylene or polyethylene laboratory material was used from the collection point of the samples to the analysis of the two compounds conforming to EPA's method.

Table 3: Physicochemical properties of PFOS and PFOA

Compounds	Molecular Formula	Molecular Weight (g/mol)	Molecular Volume (cm^3/mol)	Water Solubility (g/L)	pKa
PFOS	$C_8F_{17}SO_3K$	538	257[a]	7.5[b]	-3.27[b]
PFOA	$C_7F_{15}COONa$	414.7	226[a]	13.6[b]	0.5[b]

[a] (Xu et al., 2018)

[b](Rodea-Palomares et al., 2012)

3.3 Membrane Selection and Characteristics

The NE70 polyamide nanofiltration membrane (NE-4040-70, TCK Membrane America Inc.) was selected for this study. This thin-film composite polyamide membrane is classified as a loose membrane and suited for surface and groundwater applications. Zeta potential measurements at pH 7 in 10 mM KCl solution by Lee et al, (2010) suggest that NE70 has a negatively charged surface. NE70 has a molecular weight cutoff (MWCO) of 350 Da (Table 4), which is less than the molecular weights of the selected PFOA and PFOS (Table 3). The membrane NF270 which showed significant removal of PFAS in previous studies is tighter than NE70 with a MWCO of 200-300 Da (Kim et al., 2007). The use of a looser membrane allows for the assessment of water

matrix components interactions with contaminant rejection. Additionally, NE70 has a higher contact angle of 54.1° (Sadmani et al., 2014) as opposed to 25.2° for NF270 (Kim et al., 2007). Such parameters indicate high hydrophobicity for membrane NE70.

Table 4: NE70 membrane characteristics

Membrane	Material	Pure Water Permeability (L m^{-2} day^{-1} kpa^{-1})	Zeta Potential at pH 7(mv)	Molecular Weight Cutoff (Da)
NE70	Polyamide thin-film composite[a]	2.9[c]	-60 ±0.7[b]	350[b,c]

[a] (Chon et al., 2012)

[b] (Lee et al., 2010)

[c] (Moon et al., 2010)

3.4 Membrane Filtration Setup

The membrane filtration setup used was the CF042 crossflow acrylic cell assembly (Sterlitech Corp.,Kent,WA,USA) equipped with a 1.5-gallon feed tank. The flat sheet membranes were precut and stored at room temperature in deionized water (DI) for at least 24 hours before testing. The crossflow unit was cleaned in between uses with soap water and rinsed at least 3 times with distilled water before placing the precut membrane in the cell. The membrane was compacted with DI for at least two hours. Then, the system was drained out, filled with the 1 µg/L spiked sample mixture of PFOA and PFOS. The feed water temperature was maintained at 25± 0.5°C using a chiller unit and the permeate and concentrate were recycled back in the feed tank during the experiment. Finally, the permeate and feed were collected in 250 ml polypropylene bottles after 20 hours and placed in a 4°C refrigerator or extracted directly. Figure 5 illustrates the cell flow

diagram of the flat sheet unit. The permeate flux was calculated each time samples were collected, including at time T=0. The water flux rate (J) is defined as the flow rate(V/t) per membrane unit area (A):

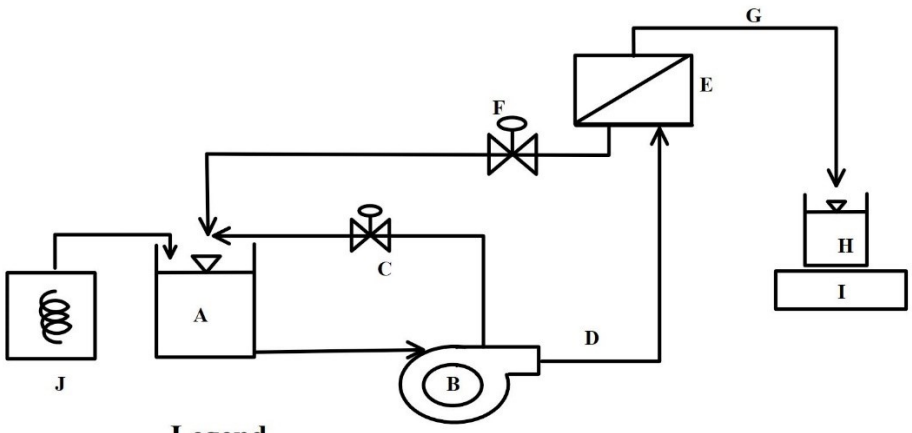

Legend

A: Feed Tank
B: Pump
C: Bypass valve
D: Flow line into the cell
E: CF042 Acrylic cell
F: Concentrate valve
G: Permeate line
H: Permeate
I: Balance
J: Chiller unit

Figure 5: CF042 cell flow diagram

$$J = V/At \quad (3.1)$$

The system recovery (r) or permeate recovery rate is the rate of conversion of the feed flow into the permeate (Q_p):

$$r = 100\% \ (Q_p / (Q_f) \quad (3.2)$$

$$Q_f = Q_p + Q_c \quad (3.3)$$

Where Q_c is the concentrate flow

The membrane removal efficiency was defined as a function of measured feed and permeate concentration:

$$R\ (\%) = (1 - (C_p / C_f)) \times 100 \quad (3.4)$$

Figure 6 shows the membrane system set up used for the flat sheet testing in the current study.

Figure 6: Bench scale flat sheet membrane system

3.5 Analytical Instruments and Extraction Equipment

3.5.1 Solid Phase Extraction

Samples were collected in 250 ml polypropylene bottles, held below 6 ℃ and extracted less than 7 days after collection date. Solid phase extraction (SPE) cartridges containing styrene divinyl-benzene (SDVB) sorbent phase (Agilent, Santa Clara, CA) were used on an extraction manifold (Waters Corporation, Milford, MA). The cartridges were first conditioned with 15 mL of LC/MS grade methanol followed by 18 mL of distilled water. Next, samples were vacuumed through the cartridges at a pressure below 20 psi and an average speed within 10-15 mL/min. The vaccum manifold apparatus is shown in figure 7 using polyethylene sample delivery tubes (Polyconn, MN.).

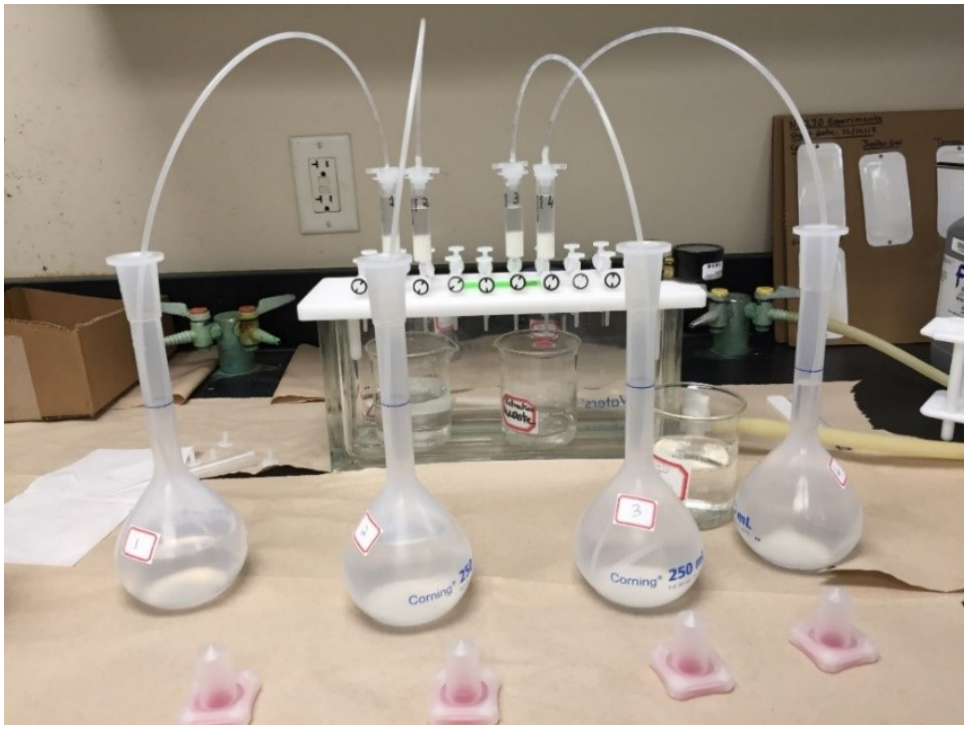

Figure 7: Vacuum manifold apparatus used for SPE

Then, the cartridges were washed with 15ml of distilled water and eluted with 8 ml of methanol. Finally, the extracts were concentrated to dryness under a stream of Nitrogen gas paired with a water bath at 45 ℃ (Organomation Associates, Inc.). The final extract matrix was a methanol: water mixture (96:4). The samples were reconstituted to obtain a final sample volume of 1 ml. More information on the sample preparation and extraction procedure are found elsewhere (Shoemaker et al., 2009).

3.5.2 LC/MS Analysis

The different water matrices were spiked with the stock solution for a target of 1 µg/L of PFOA and PFOS. The permeate and feed samples were collected after membrane testing and extracted as described in section 3.5.1. The extracts were analyzed in a liquid chromatography-tandem mass spectrometry instrument equipped with an Accucore C18 LC column (Length 100 mm x I.D. 2.1mm x Particle size 2.6 µm) preceded by a Hypersil GOLD ™ C18 reversed phase analytical column (Length 50 mm x Diameter 2.1 mm x Particle size µm), (Thermo Fisher Scientific, MA, USA). The extracts were separated using liquid chromatography, sprayed into the negative electrospray ionization source for both compounds and quantified using mass spectrometry.

3.5.2.1 LC/MS Method Development

The Thermo Scientific™ Ultimate™ 3000 Basic Manual liquid chromatography system was used to develop a method for the analysis of PFOA and PFOS. The LC was operated at a flow rate of 0.3 ml/min for a method duration of 37 minutes per injection with a 20 mM ammonium acetate (A) and a pure 100% methanol mobile phase (B). As recommended by EPA's method 537, the gradient elution was set at 60% mobile phase A and 40% mobile phase B. Compound optimization

was performed per analyte by infusing each PFA into the TSQ Qantum™ Access MAX Triple Quadrupole Mass Spectrometer by Thermo Scientific™ (MA, USA). PFOA was optimized with a single mass transition of 369.4 m/z. On the other hand, a wide range of quantitation mass transitions (m/z 499→m/z 80) was retained for PFOS as an attempt to reduce PFOS bias as required by (Shoemaker et al., 2009). The analyte infusion step was followed by the run of a mid-level calibration standard to confirm the retention times of each analyte. Figure 8 illustrates the typical peaks observed for a mid-level calibration standard (50 ng/ml) for each analyte.

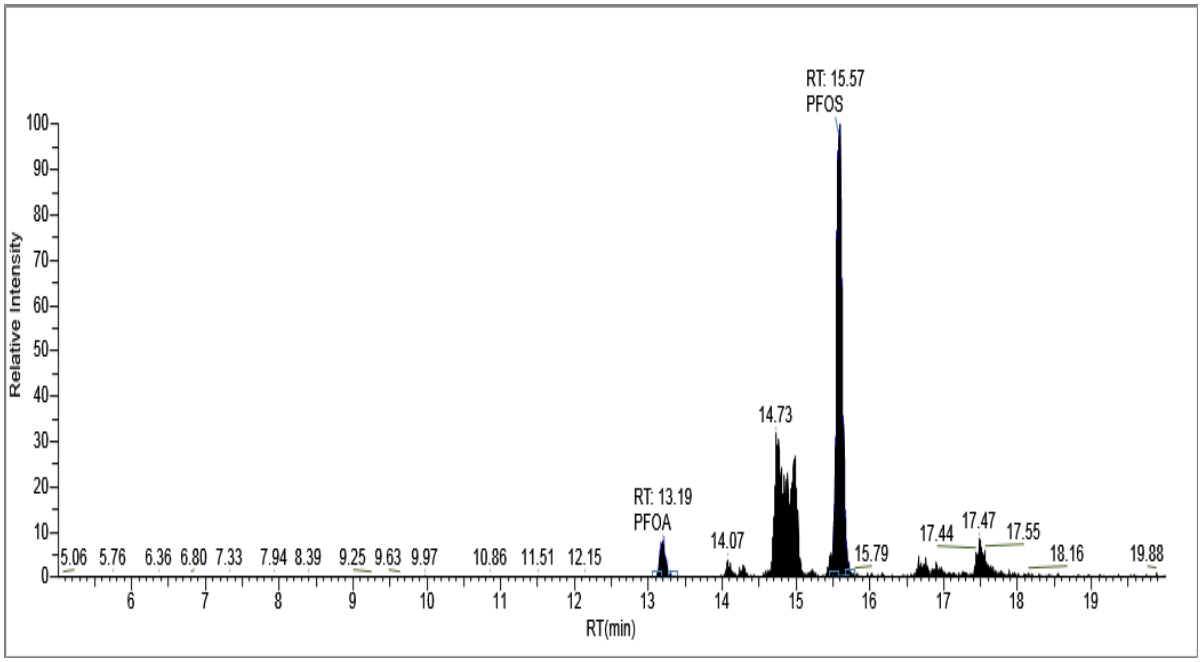

Figure 8: LC/MS chromatogram report for a mid-level calibration standard: single and double quantitation transitions peaks for PFOA and PFOS as detected by the LC/MS.

A quarterly instrument calibration was performed after the initial method development phase to ensure proper ionization conditions as described in Table 5.

3.5.2.2 Quality Assurance and Control

Prior to sample analysis, a control chart for accuracy and a method detection limit (MDL) were established for PFOA and PFOS.

Table 5: Ion source conditions during negative mode calibration

Device	Negative Mode
Spray Voltage	3000
Vaporizer Temperature	0
Sheath Gas Pressure	10
Ion Sweep Gas	0
Aux Gas Pressure	0
Capillary Temperature	270

A set of 7 replicates were obtained by spiking a known concentration (100 ng/L) of each analyte in laboratory fortified blanks (LFB). The samples were extracted and analyzed, and the mean concentration (X_{AVE}) and standard deviation (s) were obtained. The measured concentrations were calculated using a 6-level calibration curve. Equations (3.5-3.8) were used to develop a control chart for accuracy

$$UCL = X_{AVE}+3s \quad (3.5)$$

$$LCL = X_{AVE}-3s \quad (3.6)$$

$$UWL = X_{AVE}+2s \quad (3.7)$$

$$LWL = X_{AVE}-3s \quad (3.8)$$

Table 6: Method detection limit for LC/MS instrument

Sample N°	Volume (ml)	Concentration (ng/L)	
		PFOA	PFOS
1	250	81.2	66.6
2	250	71.8	64.4
3	250	128.6	75.6
4	250	81.2	126.6
5	250	76.4	79.3
6	250	80.8	71.9
7	250	79.7	73.5
Standard Deviation		19.3	21.3
Student's t		3.143	3.143
DETECTION LIMIT (ng/L)		**60.5**	**66.9**

The detection limit was obtained from the same data set by multiplying the standard deviation by the student's t parameter for 7 replicates as shown in Table 6.

Equation (3.5) allowed to calculate the mass recovered by the LC/MS after each sample injection.

A spike recovery chart was established in Figure 9 using the recoveries of 7 replicates per analyte. Analyte recoveries for the replicates analysis ranged from (64.4%- 128%). The minimum reporting level, defined as the lowest concentration at which the recoveries will fall within 50-150%, was established at a target of 100 ng/L.

$$\text{Percent Recovery} = \frac{\text{Measured Mass}}{\text{Mass Added}} \times 100 \qquad (3.9)$$

Following the MDL analysis, the mean and standard deviation of seven replicates were used to predict with 99% confidence the upper and lower prediction interval of results. The upper and lower limits fell within 50-150 % recovery, hence confirming the target reporting level of 100 ng/L.

For each new set of SPE cartridges, a laboratory reagent blank (LRB) was extracted along with samples. A field blank was also extracted and analyzed for each water matrix collected. Prior to each flat sheet test, DI water was conducted into the system with no membrane to ensure contributions from the bench scale set up were negligible. Polyethylene tubing was installed in the membrane filtering unit to minimize adsorption of compounds and contamination. Duplicate and replicate samples were obtained and analyzed for every 10 samples in the running batch. The relative standard deviation (RSD) was calculated using Equation (3.6). The duplicates and replicates analyzed for this study showed RSD values within (2-17%).

$$\text{RSD} = \frac{s}{X_{AVE}} \times 100\% \qquad (3.10)$$

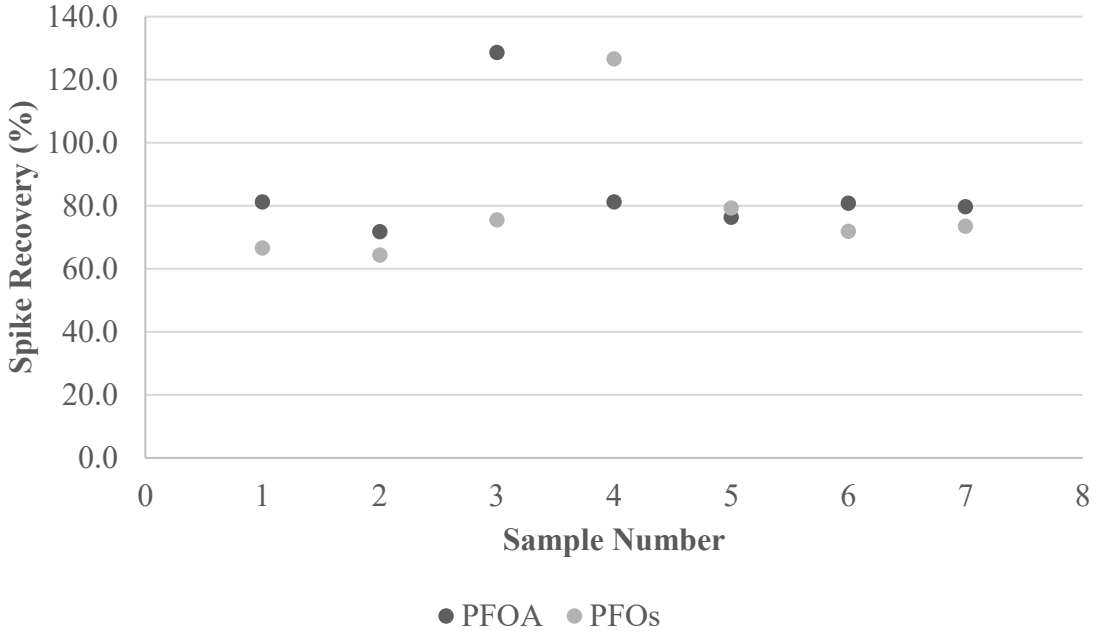

Figure 9: Spike recovery chart for PFOA and PFOS detected by LC/MS

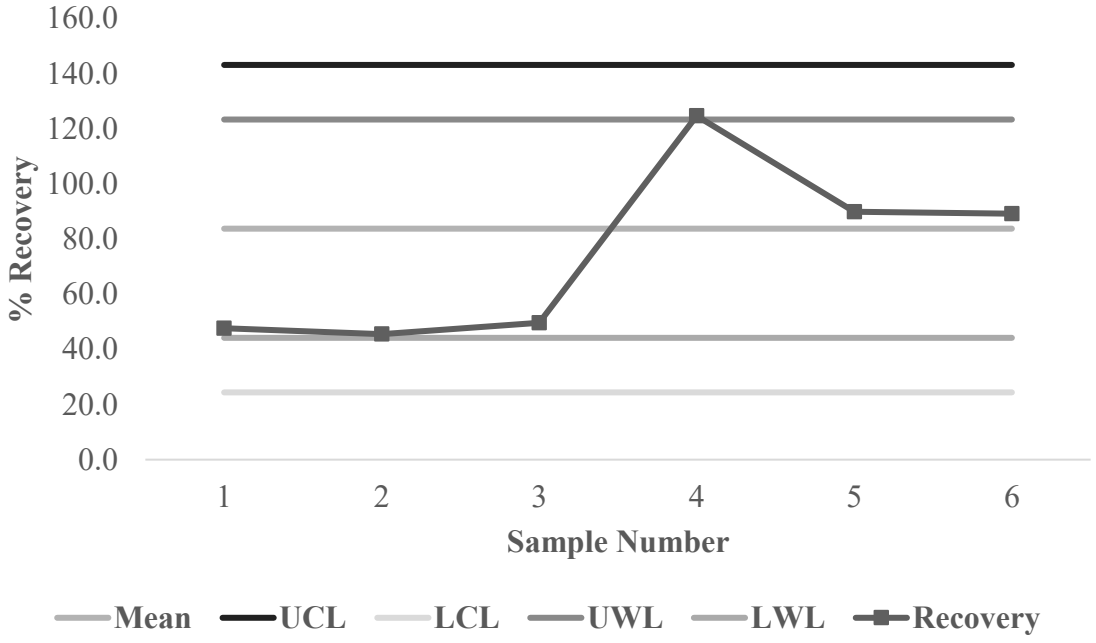

Figure 10: Control chart for accuracy: control, surface and groundwater feed water samples spiked at 1µg/L

The accuracy of the data was confirmed by plotting spiked samples recoveries in the control chart for accuracy. The data met the accuracy criteria with no control chart violations as shown in Figure 10.

3.5.3 Matrix Component Characterization

The pH, alkalinity, conductivity, turbidity and TDS of the water matrices were measured in the UCF drinking water research laboratory to distinguish the characteristics of each water. After collection, the water quality parameters were obtained based on standard methods ("Standard Methods for the Examination of Water and Wastewater," 2012).

3.5.3.1 Dissolved Organic Carbon (DOC) Analysis

The DOC content in the water samples was measured prior to performing flat sheet testing. DOC is the fraction of the total organic matter that passes through a 45µm filter. The Fusion Total Carbon Analyzer (Teledyne Tekmar Inc, Mason, OH) was used for DOC measurement in accordance with standard methods The method detection limit for this instrument was established at 0.25 mg/L.

3.5.3.2 Specific Ultraviolet Absorbance (SUVA)

The UV absorbance at 254 nm was analyzed using a DR5000 spectrophotometer (Hach, Loveland, CO). The specific absorbance is obtained from dividing the absorbance of a sample at a wavelength of 254 nm by the DOC content. Samples were filtered through a 45µm filter prior to loading a cuvette for analysis in the spectrophotometer.

3.5.3.3 Inductively Coupled Plasma Spectrometer (ICP)

The cations concentration measurements were carried out using an ICP spectrometer (Perkin Elmer Optima, MA) according to standard methods 3120 B. The samples were filtered using a 45µm filter and digested using concentrated nitric acid before analysis. A standard curve generated using certified calcium and magnesium standards was used to estimate the concentration of calcium and magnesium ions in the samples.

CHAPTER 4. RESULTS AND DISCUSSIONS

4.1 Bench-Scale Nanofiltration Experimental Parameters

The membrane system recovery was initially set at a range of 3±0.4% for the three experimental runs.

Table 7: Bench scale flat sheet system operating parameters (T= 0 hr.)

Parameter	Water Matrix		
	Control	**Ocmulgee River**	**Jupiter Groundwater**
Initial Permeate Flow Rate (Q_p) (ml/min)	3.53	3.95	4.03
Transmembrane Pressure (Psi)	87	87	87
Initial Membrane Flux (J) (ml/min/m^2)	841	940	960
Concentrate Flow Rate (Q_c) (ml/min)	129	129	129
Feed Flow Rate (Q_f) (ml/min)	132	133	133
Initial Recovery (%)	3±0.4	3±0.4	3±0.4
Final Recovery (%)	2±0.6	2±0.6	2±0.6

The system was allowed to equilibrate for 20 hours in recycling mode and the final recovery (2±0.6)% was determined using the final permeate flux during permeate and feed samples

collection. The initial membrane flow rate was recorded for each run and the initial flux was calculated based on a membrane active area of 42 cm^2. The concentrate flow rate was maintained at a constant rate of 129 ml/min for the three runs. The temperature of the feed water was maintained at 25±0.5°C.

4.2 Compound Rejection of PFOA and PFOS: Three Water Matrices Examined

The compounds rejection varied between 71-80% for PFOA and 42-80% for PFOS by the NE70 membrane tested (Figure 11). Many literatures observed greater than 90% removal for PFOA and PFOS using NF270 membranes (MWCO 200 Da) (Hang et al., 2015; Pramanik et al., 2017). Lower removal efficiencies were expected using NE70 based on the MWCO of the membrane (MWCO 350 Da). While PFOS has a higher molecular weight (MW = 538 g/mol) than PFOA (MW= 436 g/mol), lower rejection (by up to 28.4%) of PFOS compared to PFOA in the three matrices was observed. These results suggest that size exclusion based exclusively on compound molecular weight may not be the governing removal mechanism. The groundwater, containing higher cations (122 mg/l Ca^{2+} and 5 mg/l Mg^{2+}) and organic matter (10 mg/l), exhibited higher removal (80%) for both PFOA and PFOS compared to the DI and surface water. These findings indicate that water matrix components play an important role in the rejection of PFOS and PFOA byNF due to compound interactions with water constituents (e.g., DOM and cations) and the membrane. Similar results were found in studies investigating PFOS removal in water matrices with high cations (calcium and magnesium) content as discussed in the following section (Zhao et al., 2016).

Table 8: PFOA and PFOS rejection using NE70 membrane

Compound	NE70 Membrane Rejection (%)		
	Control	Ocmulgee River	Jupiter Groundwater
PFOA	71.3	78.6	80.4
PFOS	42.6	65.6	80.3

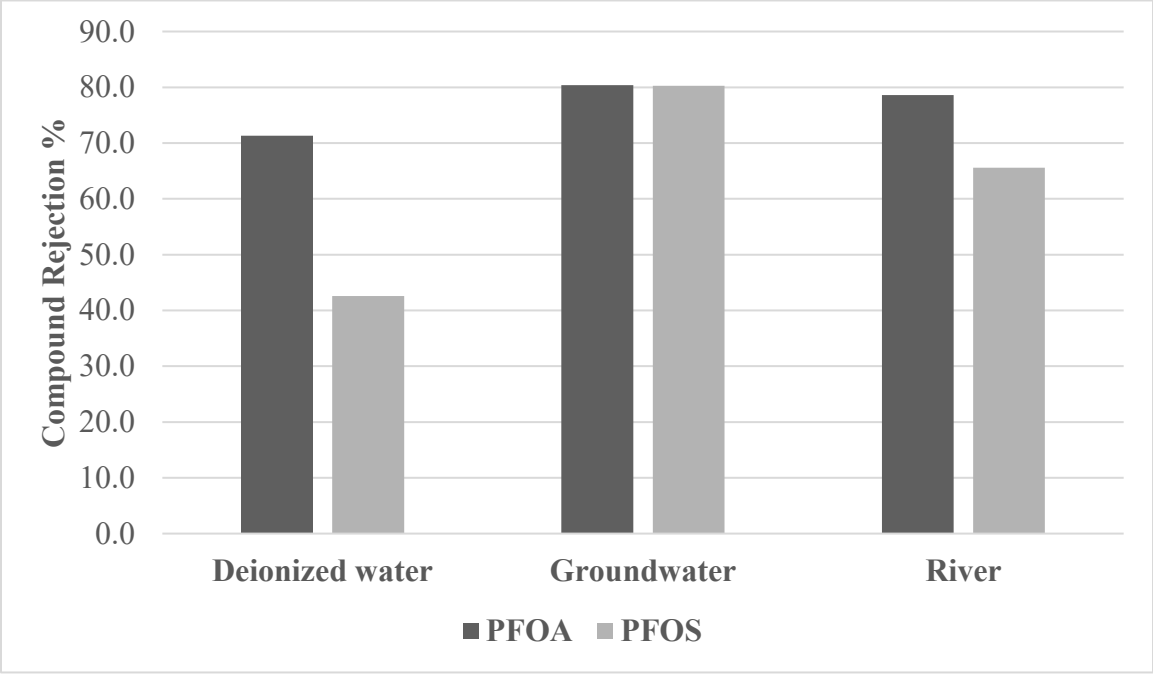

Figure 11: PFOA and PFOS rejection as a function of matrix type

4.2.1 Effect of Cations Concentration on Rejection of PFOS

The effect of calcium and magnesium ions on the rejection of PFOA and PFOS was investigated. An increasing trend in PFOS rejection was observed as the calcium and magnesium concentrations increased in the water matrix. A less noticeable trend was observed with PFOA rejection in both cases. The impact of matrix components on PFOA rejection is addressed in section 4.2.4. Studies have shown that PFOS removal was enhanced by the presence of cations in the feed water due to the presence of sulfonate groups in their molecular structure. Zhao et al., (2018) attributed this to the bridging between cations and PFOS molecules and further demonstrated the formation of a complex with one PFOS molecule PFOS-Cation$(H_2O)_4$ and/or two PFOS molecules $(PFOS)_2$-Cation$(H_2O)_2$.

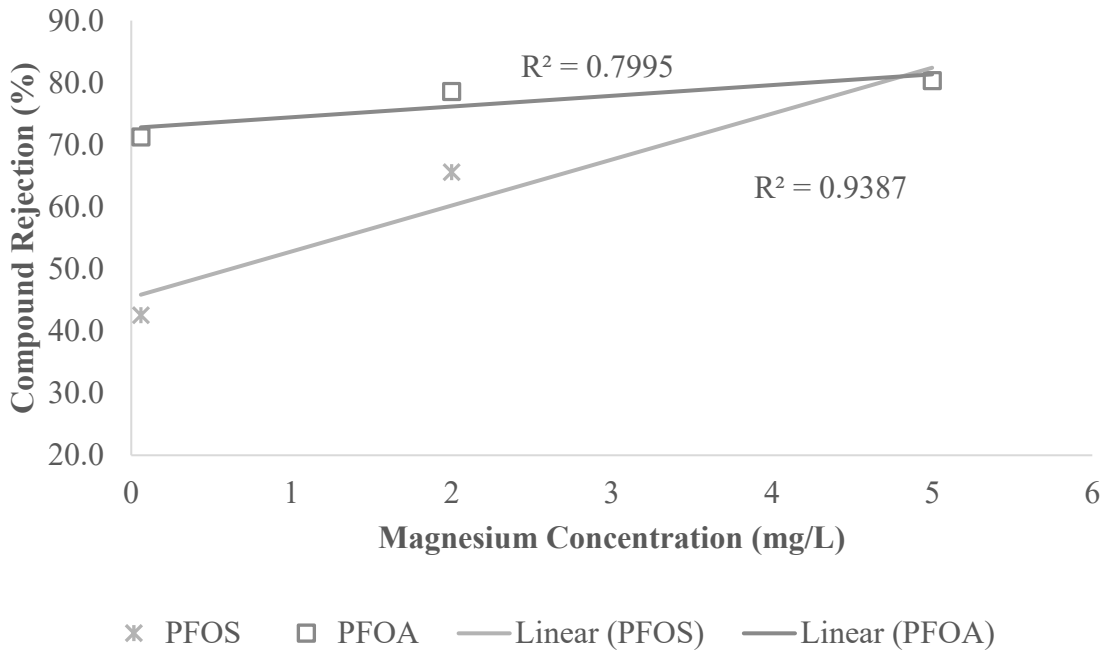

Figure 12: Compound rejection as a function of magnesium ion concentration

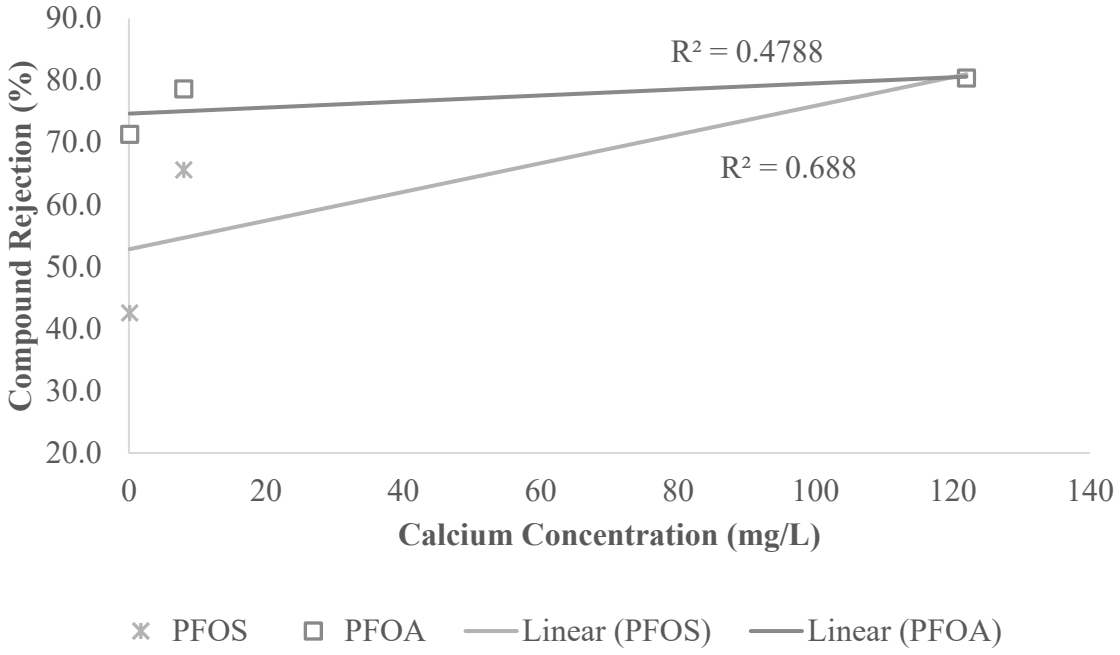

Figure 13: Compound rejection as a function of calcium ion concentration

Hence, the new PFOS-cation complex accumulates on the membrane surface, creating a sieving effect that promotes PFOS rejection. Similar findings linked enhanced PFOS removal to complexation effect of cations (F. Wang et al., 2011). Figure 12 depicts the strong correlation (r^2= 93.9%) between the rejection of PFOS and the magnesium concentration. Zhao et al., (2016) demonstrated similar effects with magnesium ions under different operating pressures. An increasing PFOS removal trend was also noted for calcium ions in Figure 13.

4.2.2 Effect of DOC on Rejection of PFOS

The river and groundwater matrices examined contained higher organic content than the laboratory reagent water. As these matrices were more efficient in removing PFOA and PFOS compared to deionized water, the effect of DOC was investigated on the rejection of the two PFAS (Figure 14).

A few studies noted the interactions between natural organic matter and PFOA and PFOS (Xiao et al., 2013). Comparably to the effects of cations, the deposition of organic particles on the membrane may cause a fouling layer that reduces the passage of PFOs and PFOA molecules, through the membrane. Appleman et al., (2013) indicated increased NF rejection with the presence of a fouling layer caused by organic matter present in wastewater.

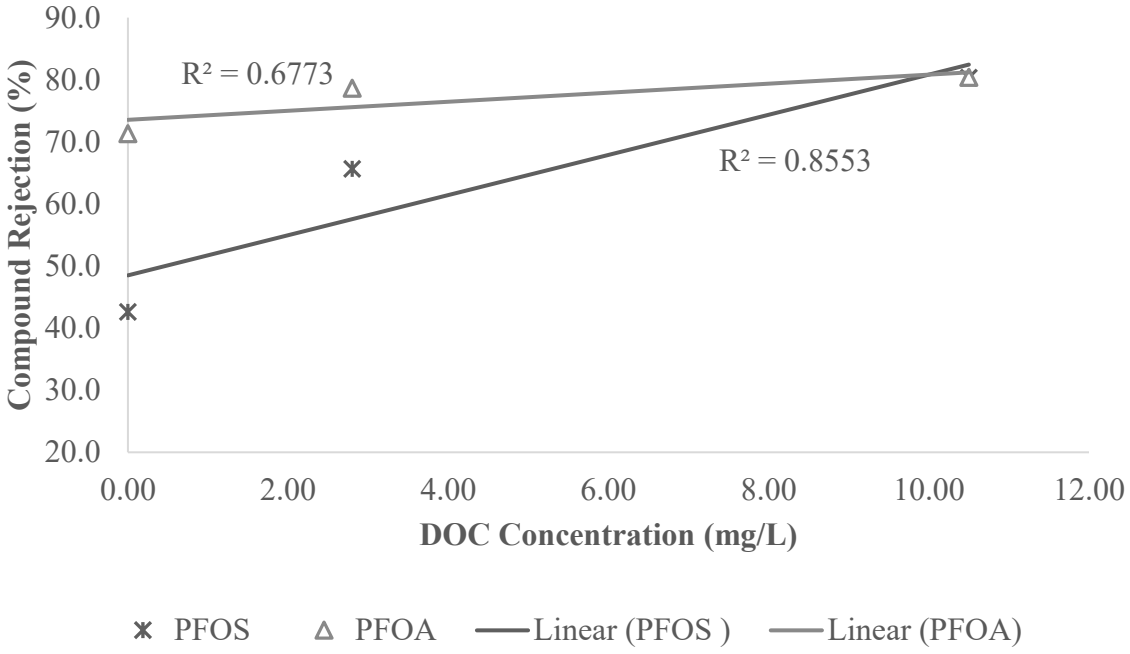

Figure 14: Influence of DOC concentration on the removal of PFOS and PFOA

4.2.3 Effect of Flux Decline

A decline in permeate flux over time was observed for the conducted experiments. The evidence of a decrease in permeate flux in the control experiment suggests PFOS sorption on the membrane as asserted by (Steinle-Darling et al., 2008). The deposition of cations and natural organic matter on the membrane surface as explained in sections (4.2.1 and 4.2.2) also facilitates the formation

of a blocking layer resulting in a flux decline. Tang et al., (2007) suggested that the dissolution of PFOS in the membrane polyamide layer might likely block solute and water diffusion, hence reducing the flux over time. The same effect was observed when using NF to remove PFOA from groundwater and PFOA-spiked deionized water with flux declines of 32.8% and 5.3 % respectively (Boonya-atichart et al., 2016).

Table 9: Flux decline observed after 20 hour run with a transmembrane pressure of 87 Psi

Parameters	**20 Hour Flat Sheet Test**		
	Control	**Ocmulgee River**	**Jupiter Groundwater**
Transmembrane Pressure (Psi)	87	87	87
Flux Decline (%)	12.3	27.6	56.2
Permeate Recovery (%)	2±0.6	2±0.6	2±0.6

While flux decline may originate from foulant enhanced concentration polarization (Steinle-Darling et al., 2008), consequently decreasing PFOS rejection, adverse effects were observed in the present study. As shown in Figure 15, PFOA and PFOS rejection increased with declining flux. This trend was also demonstrated by Appleman et al., (2013). A flux decline of 50% was reported by Zhao et al., (2016) when 10 mg/L of humic acid was added in the feed solution containing PFOS. The flux declined further when Mg^{2+} was added, suggesting that Mg^{2+} may facilitate intermolecular bonding between humic acid and the membrane. Another cause of flux reduction might be the precipitation of calcium ions leading to pore blockage on the membrane surface and

increased compound rejection. This explanation, as suggested by T. Wang et al., (2015) justifies the increased rejection for PFOA with declining flux.

4.2.4 Rejection of PFOA: Influence of Fouling and Compound Properties

Overall, matrix components' influence on PFOA rejection was less noticeable compared to PFOS. On the other hand, Figure 15 shows a significant correlation (r^2 = 91%) between flux decline and PFOA rejection. In DI water, where a flux decline of 12.3% was indicated despite lower DOC and cations concentration, the hindered water passage across the membrane resulted in more PFOA retention. These findings may be associated with the compound properties of PFOA.

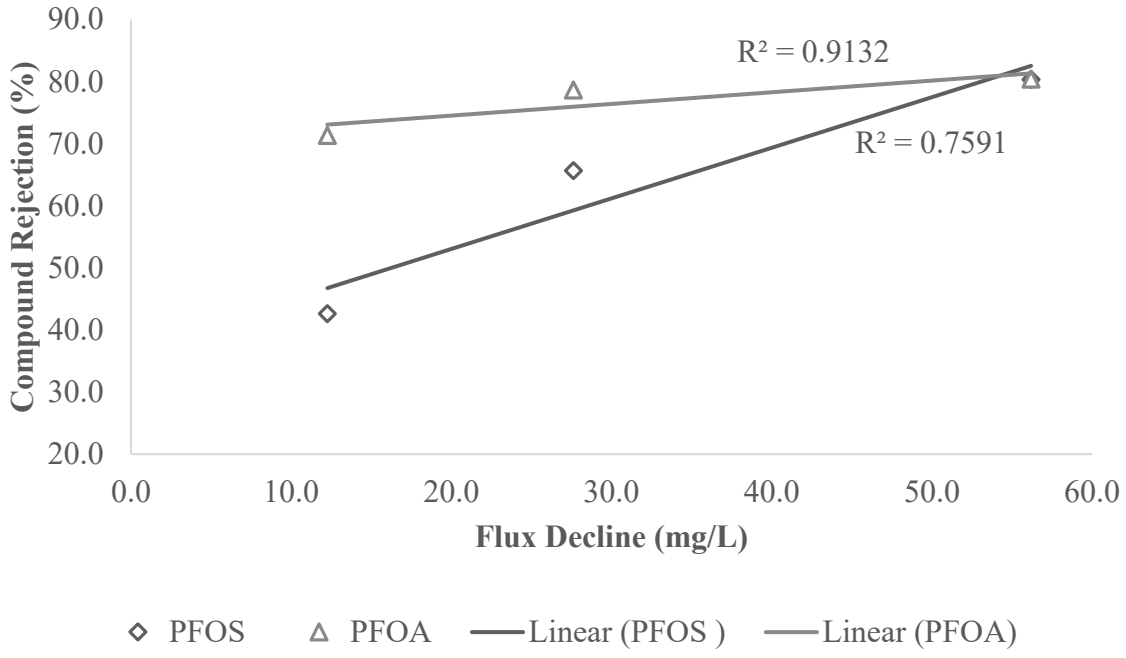

Figure 15: Effect of flux decline on the rejection of PFOS and PFOA

Whereas both PFOS and PFOA showed efficient sorption properties to sediments and adsorption media, Ahrens et al., (2011) indicated that PFOA can easily desorb from organic sediments to the

aqueous phase in marine environments. The lack of sorption sites due to the presence of bigger size molecules (PFOS, NOM and PFOS-cation complexations) on the membrane, combined with the higher water solubility of PFOA may have caused higher PFOA rejection in the three waters tested in this study.

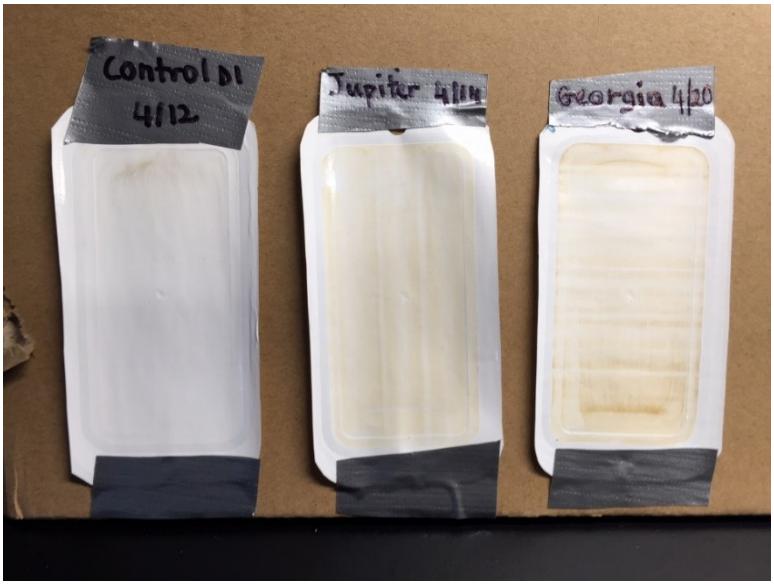

Figure 16: Used NE70 membranes for the control (deionized water), Jupiter (groundwater) and Ocmulgee river (Georgia)

4.3 Correlating Flux Decline with Matrix Constituents Using Pearson's Correlation

To further evaluate the significance of the trends observed in section 4.2, the MINITAB statistical software package was used to obtain correlation parameters and perform regression analysis across various matrix variables. Pearson's correlation evaluation was used to determine linear relationships within the set of parameters at a confidence level of 95%. Water matrix components including DOC, cations (Ca^{2+} and Mg^{2+}) and flux decline were tested for correlation with rejection. MINITAB provided Pearson correlation (r) and p values summarized in Table 10.

Table 10: Pearson correlation and p values for selected matrix components and permeate flux

	DOC mg/L	Ca mg/L	Mg (mg/L)	UV254
Flux Decline (%)	0.981	0.923	0.999	0.907
P value	**0.001**	**0.009**	**0.000**	**0.012**
Rejection	0.662	0.587	0.698	0.570
P value	0.152	0.220	0.123	0.237

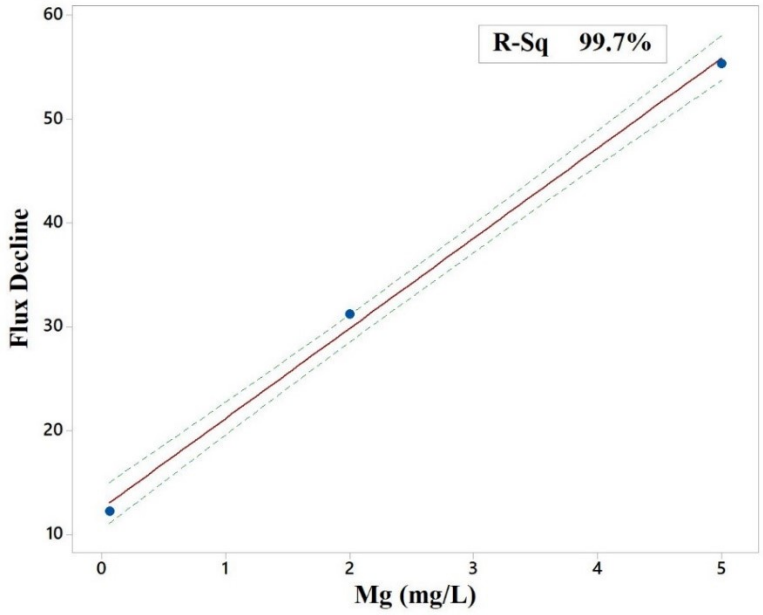

Figure 17: Flux decline with increasing magnesium ion concentration

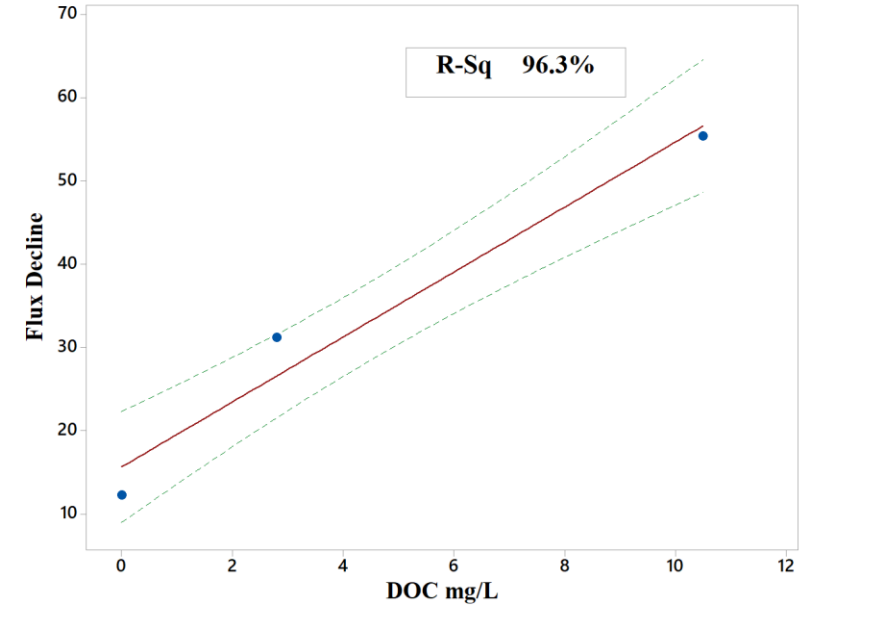

Figure 18: Flux decline with increasing DOC concentration

Statistically significant correlations with a p value less than $\alpha = 0.05$ were captioned in bold. A strong relationship was shown between membrane flux decline and water matrix components. Particularly, a Pearson correlation value of 99.9% suggested that magnesium ion concentration is strongly related to flux reduction (Figure 17) . r values > 98% indicated that the presence of natural organic matter in the water caused membrane fouling resulting in a flux decline (Figure 18). A less strong, but still significant correlation, was obtained between calcium ion concentration and flux decline. Altogether, the water matrix constituents played a major role in causing flux decline which further hindered solute and water passage through the membrane.

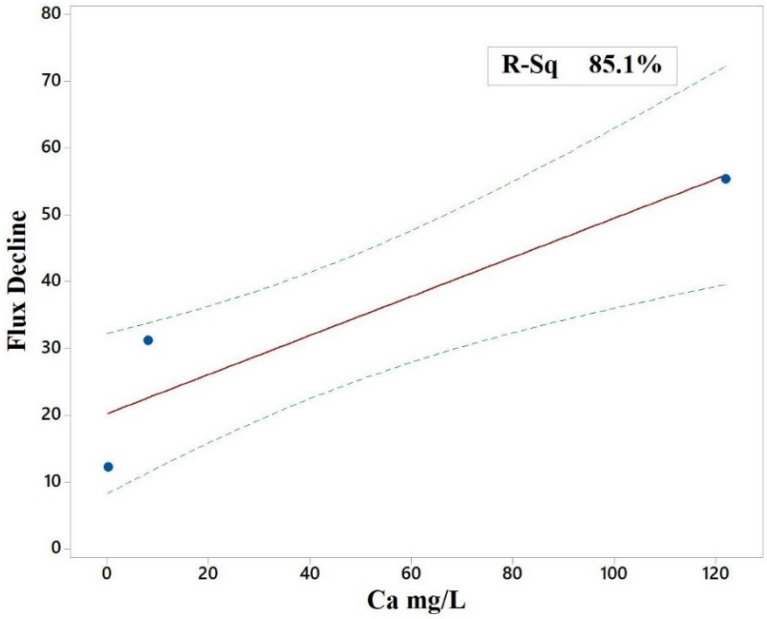

Figure 19: Flux decline with increasing calcium concentration

CHAPTER 5. CONCLUSIONS AND RECOMMENDATIONS

5.1 Impact of Matrix Components on the Removal of PFC's using NE70

The removal of PFOA and PFOS from different water sources using nanofiltration was investigated. Deionized, surface and groundwater samples were collected and fortified with a mixture of 1 µg/L PFOA and PFOS and filtered using a bench scale flat sheet set-up for 20 hours at a constant pressure. Feed and permeate samples were analyzed and a comparison of rejection values was established. The distinctive characteristics of each water matrix allowed to investigate the influence of water matrix components (dissolved organic matter and cations such as Ca^{2+}, Mg^{2+}) on the rejection of perfluorinated compounds.

5.1.1 Factors Influencing the Removal of PFOA

Higher PFOA rejection (71.3%), compared to PFOS (42.6%) was observed in DI water, where the impact of organic matter and cations was less observable. Overall, the direct correlation between cations and PFOA rejection was less significant than PFOS. Such results suggested that PFOA is less likely to form complexes with calcium and magnesium ions in a water matrix. Nevertheless, the rejection of PFOA was mainly associated with flux decline. The higher system flux decline (56.2%) may have contributed to enhanced PFOA rejection based on the higher hydrophilic properties of PFOA. Moreover, the enhanced PFOA rejection may be due to its higher water solubility ($9.5x\ 10^3$ mg/L at 25°C) as opposed to 680 mg/L for PFOS (USEPA, 2016). The noted impact of flux decline on the PFOA rejection suggests that the sieving effect plays an important role in the nanofiltration of perfluorinated compounds.

5.1.2 Factors Influencing the Removal of PFOS

Unlike PFOA, water matrix properties had a significant influence on PFOS. Increased rejection with increasing DOC and cations concentration were recorded in the case of PFOS. Flux decline also played a significant role on both compounds rejection. Strong correlation values suggested that the flux decline was not only caused by the membrane fouling due to the deposition of foulant layer on the membrane surface, but also the interactions of cations and PFOS molecules with the membrane. The presence of sulfonic groups in the molecule of PFOS may favor the interactions between cations and PFOS. Several mechanisms could be attributed to the enhanced PFOS rejection in presence of DOC and cations:

1) The accumulation of the larger molecules from complexation of PFOS-Cations molecules on the membrane surface may cause hindered solute and water passage. $Ca^{2+}$and Mg^{2+}ions may act as bridging agents between two PFOS molecules resulting in higher rejection.
2) The presence of organic matter, combined with cations may result in intermolecular bridging between DOC and $Ca^{2+}$and Mg^{2+} ions, consequently forming a fouling layer on the membrane surface.

In both cases, the enhanced PFOS rejection is likely due to the accumulation of organic particles on the membrane surface, consequently creating a sieving effect.

5.2 General Conclusions

The variety of natural water matrix components has a major effect on the rejection of perfluorinated compounds by nanofiltration. Unlike many studies that reported charge repulsion

as the governing removal mechanism of perfluorinated compounds, the presence of matrix components such as dissolved organic matter, and $Ca^{2+}$and Mg^{2+} ions impacted the transport/rejection of PFOA and PFOS during nanofiltration. Improved rejections in natural water matrices further suggest compound complexations with water constituents, mainly in the case of PFOS. The understanding of the complex interactions of PFOA and PFOS will lead to significant contributions to the efforts of protecting aquatic environments and consequently public health.

Various literatures mentioned in the current study have performed laboratory experiments on the removal of PFCs via NF. Many studies featured artificial source waters as a feed solution and the use of a bench-scale NF unit. For practical applications, future investigations should ensure the use of more natural water sources, as opposed to synthetic, to account for the influence of matrix components on compound rejection. The experiments in the current document were performed at low recoveries (~3%) due to limitations in equipment. Although such recovery may be realistic for a single membrane element of 42 cm^2 of active area, more research should be oriented towards the use of pilot nanofiltration plants, which have a greater ability to mimic full-scale systems. The use of more performant bench-scale or pilot nanofiltration systems may minimize the impact of system operations factors (such as a decline in system recovery) on the rejection of the compounds.

The current study has shown that cations and DOM play a significant role on the rejection of PFOA and PFOS by nanofiltration. To provide further insights on the intermolecular interactions of matrix constituents with the PFCs, previous studies have demonstrated the usefulness of molecule geometry simulations such as the Density Functional Theory (DFT). The study of the bonding capacity of PFCs at the molecular level is crucial to reduce their impacts in environmental systems.

In addition, membrane characterization parameters of virgin and fouled membranes may further show changes in the membrane surface properties due to the presence of matrix components.

APPENDIX A: LC/MS CALIBRATION CURVES

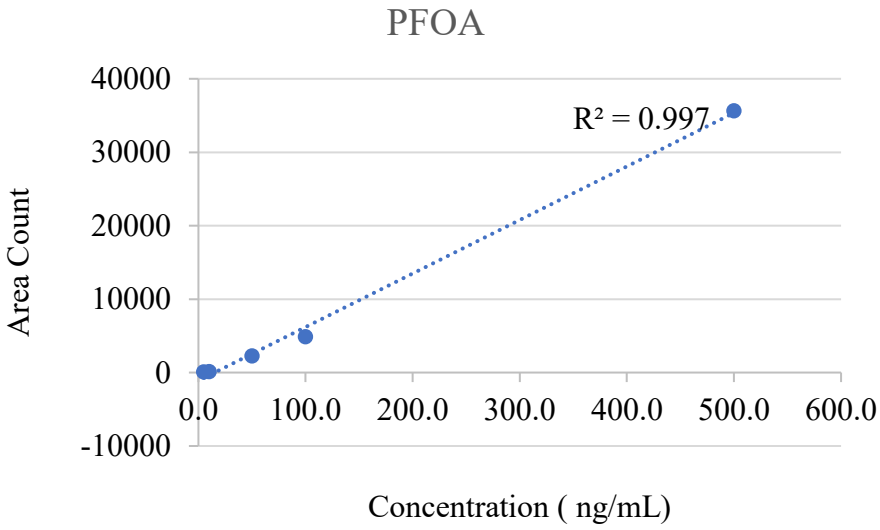

Figure 20: Detection limit: calibration curve for PFOA

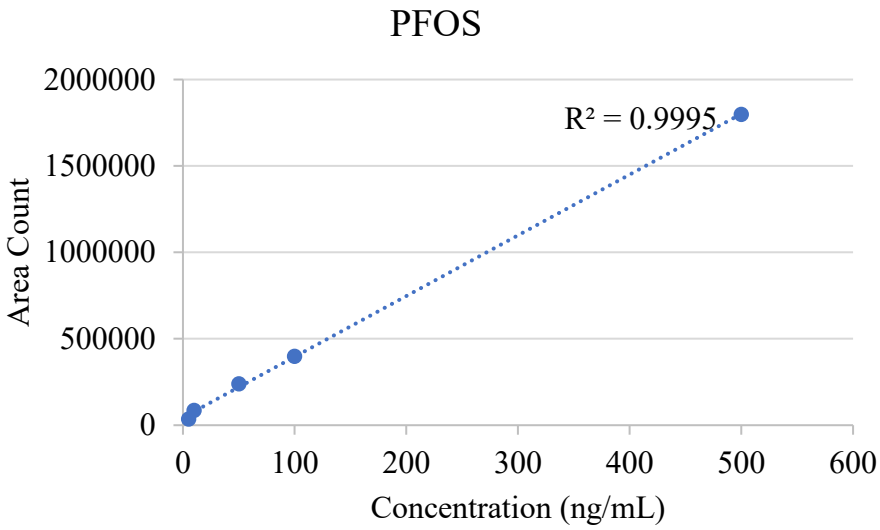

Figure 21: Detection limit: calibration curve for PFOS

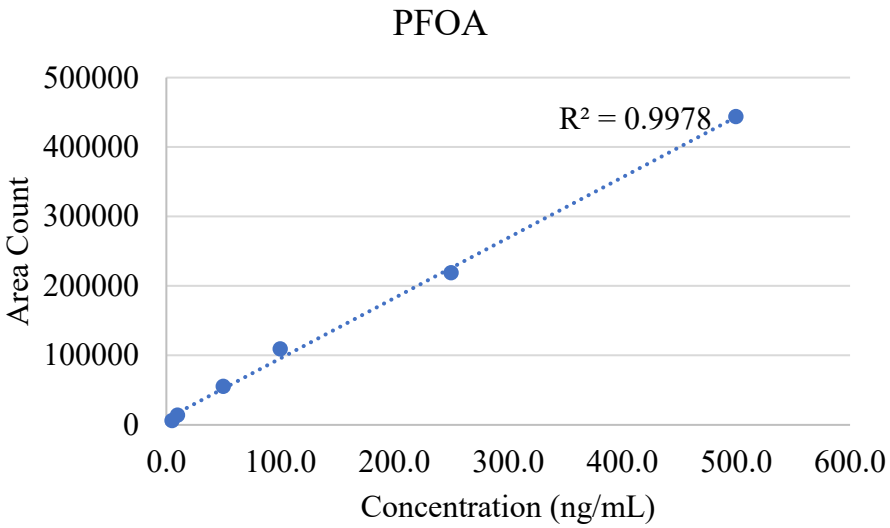

Figure 22: PFOA calibration curve for DI and groundwater samples

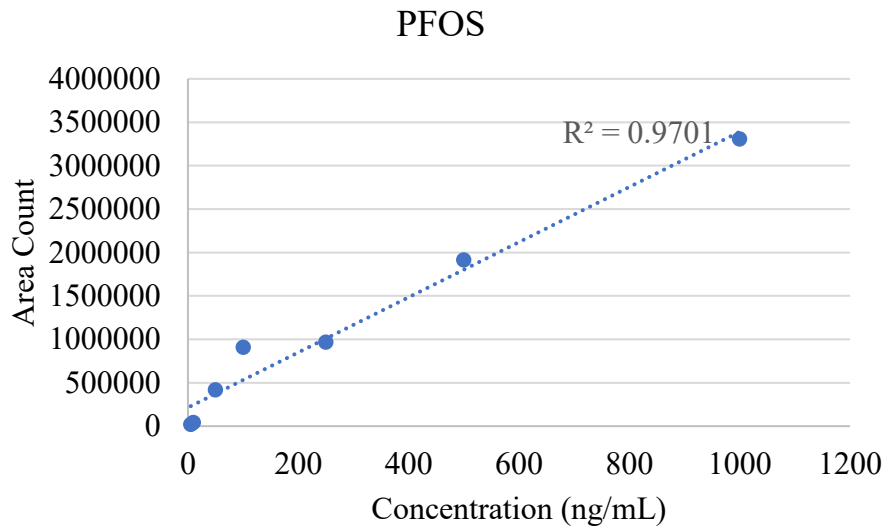

Figure 23: PFOS calibration curve for DI and groundwater samples

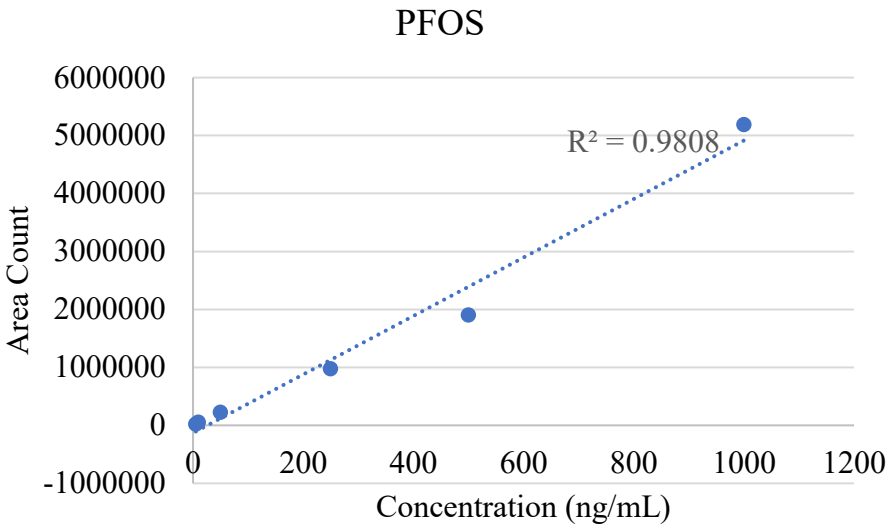

Figure 24: PFOS calibration curve for Ocmulgee river sample

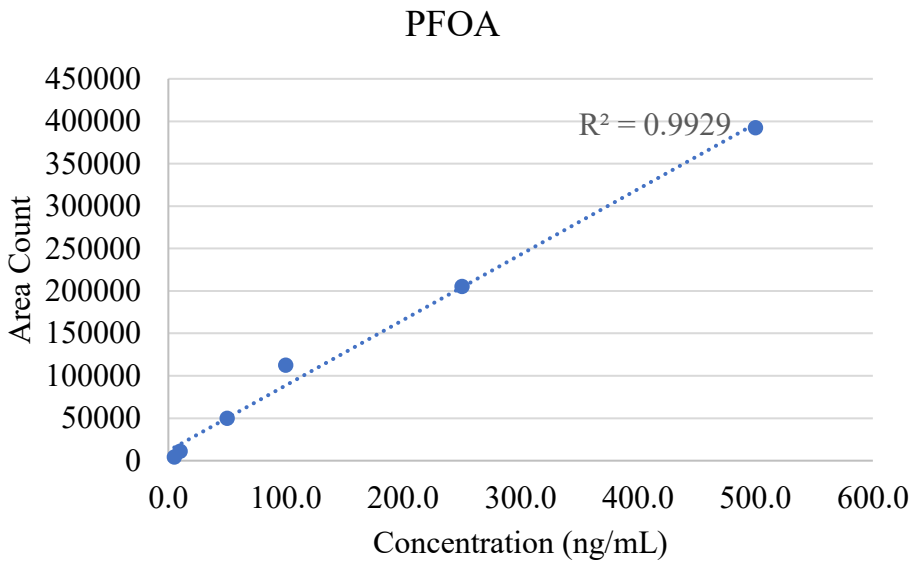

Figure 25: PFOA calibration curve for Ocmulgee river sample

APPENDIX B: LC/MS AREA COUNTS

The samples were extracted, and the area counts were obtained from the LC/MS for each injection.

Table 11: Detection limit: area counts and estimated concentrations

Sample	Volume	Area Count		Extract Concentration (ng/mL)	
	mL	PFOA	PFOS	PFOA	PFOS
1	250	380	14040	20.3	16.6
2	250	208	12128	18.0	16.1
3	250	1244	21928	32.2	18.9
4	250	380	66738	20.3	31.6
5	250	291	25197	19.1	19.8
6	250	372	18742	20.2	18.0
7	250	352	20091	19.9	18.4

The slope and y-intercept were retrieved from the regression equation and used to estimate the samples concentrations.

Extract Concentration (ng/mL)= Area Count + y-intercept/slope

Concentration (ng/L)= 1000*Concentration (ng/mL)/ 250*

*Dilution factor for a sample of 250 mL extracted and concentrated to a final volume of 1 mL.

Sample Recovery % = 100* Measured Concentration (ng/mL)/ Actual Concentration (ng/mL)

Detection Limit (ng/L) = Student's t for 7 replicates*Standard Deviation

Table 12: DI sample concentration calculations

Sample	Volume	Area count		Extract Concentration (ng/ml)		Concentration (ng/L)	
DI	**ml**	**PFOA**	**PFOS**	**PFOA**	**PFOS**	**PFOA**	**PFOS**
Blank*	250	550	14253	10.8	71.8	43.1	287
Spike/Feed 1	250	94770	776085	119	311	477	1246
Feed 2 20hr	250	114462	407630	142	195	568	782
Feed 2 D 20hr.	250	106703	427489	133	202	532	807
Permeate 1 20 hr.	250	25452	148729	39.4	114	157	456

Table 13: PFOA and PFOS rejection for DI matrix

Sample	**NE70**	
Deionized Water (ng/L)	**PFOA**	**PFOs**
Spike Feed 1	477	1246
*** Feed 2**	550	795
Permeate 1	158	456
Rejection (%)	**71**	**43**

Table 14: Area counts for calibration standards used for analysis of DI and groundwater samples

Samples	**Area Count**	
Deionized Water and Groundwater	**PFOA**	**PFOS**
C1 (5 ng/ml)	6082	21343
C2 (10 ng/ml)	13946	43220
C3 (50 ng/ml)	55604	419118
C4 (100 ng/ml)	109285	907392
C5 (250 ng/ml)	219056	965084
C6 (500 ng/ml)	443663	1915728
C7 (1000 ng/ml)	748458	3307122

Table 15: Groundwater samples concentration calculation

Sample	Volume	Area count		Extract Concentration (ng/ml)		Concentration (ng/L)	
Groundwater	**mL**	**PFOA**	**PFOS**	**PFOA**	**PFOS**	**PFOA**	**PFOS**
Feed 1	250	80923	499865	93.3	122	373	488
Feed 2 20hr	250	128653	500246	151	122	607	488
Permeate 1 20 hr.	250	30283	122705	31.2	24.0	125	96.4
Feed 3	250	112755	282752	132	65.6	529	263
Feed 3 D	250	139955	339546	166	80.4	662	322

Table 16: PFOA and PFOS rejection for groundwater sample

Sample	NE70	
Groundwater (ng/L)	**PFOA**	**PFOs**
Spike Feed 1	418	488
*** Feed 2**	636	489
Permeate 1	125	96
Rejection (%)	**80**	**80**

Table 17: Area counts for calibration standards used for analysis of river water samples

Sample: River	Area Count	
	PFOA	**PFOS**
C1 (5 ng/ml)	4100	22445
C2 (10 ng/ml)	11198	54442
C3 (50 ng/ml)	49850	224347
C4 (100 ng/ml)	112558	1037498
C5 (250 ng/ml)	205217	974623
C6 (500 ng/ml)	392132	1904786
C7 (1000 ng/ml)	699721	5188789

Table 18: Ocmulgee river samples concentration calculations

Sample	Volume	Area count		Concentration (ng/ml)		Concentration (ng/L)	
River	mL	PFOA	PFOS	PFOA	PFOS	PFOA	PFOS
Blank	250.0	20194	17295	11.1	29.4	44.5	118
Feed 1	250.0	105814	993603	122	223	489	892
Feed 1 D	250.0	108759	1141217	126	252	504	1009
Feed 2 20hr	250.0	100228	935161	115	211	459	845
Permeate 1 20 hr.	250.0	31103	235561	25.3	72.7	101	291

Table 19: PFOA and PFOS rejection for Ocmulgee river

Sample	NE70	
River (ng/L)	PFOA	PFOs
***Spike Feed 1**	496	950
Feed 2	473	845
Permeate 1	101	291
Rejection (%)	**78.6**	**65.6**

APPENDIX C: AVERAGE PERMEATE FLUX CALCULATIONS

Table 20: DI experiment: initial permeate flux

Permeate	Volume (mL)	Time (min)	Flow Rate (mL/min)	Flux (mL/min/m^2)
1	36	10.0	3.60	857
2	35	10.0	3.50	833
3	35	10.0	3.50	833
	Average Permeate Flux (mL/min/m^2)			841

Table 21: Groundwater experiment: initial permeate flux

Permeate	Volume (mL)	Time (min)	Flow Rate (mL/min)	Flux (mL/min/m^2)
1	22	5.5	4.04	961
2	23	5.5	4.18	996
	Average Permeate Flux (mL/min/m^2)			978

Table 22: River experiment: initial permeate flux

Permeate	Volume (mL)	Time (min)	Flow Rate (mL/min)	Flux (mL/min/m^2)
1	23	6.0	3.83	913
2	22	6.0	3.67	873
	Average Permeate Flux (mL/min/m^2)			893

Table 23: Final permeate flux (20 hours)

Final Flux	Volume (mL)	Time (min)	Flow Rate (mL/min)	Flux (mL/min/m^2)
DI	31	10.0	3.10	738
Groundwater	21	11.7	1.79	429
River	19	7.00	2.71	646

REFERENCES

Ahrens, L., Yeung, L. W. Y., Taniyasu, S., Lam, P. K. S., & Yamashita, N. (2011). Partitioning of perfluorooctanoate (PFOA), perfluorooctane sulfonate (PFOS) and perfluorooctane sulfonamide (PFOSA) between water and sediment. *Chemosphere, 85*(5), 731-737. doi:https://doi.org/10.1016/j.chemosphere.2011.06.046

Appleman, T. D., Dickenson, E. R. V., Bellona, C., & Higgins, C. P. (2013). Nanofiltration and granular activated carbon treatment of perfluoroalkyl acids. *Journal of Hazardous Materials, 260*(Supplement C), 740-746. doi:https://doi.org/10.1016/j.jhazmat.2013.06.033

Bellona, C., Drewes, J. E., Xu, P., & Amy, G. (2004). Factors affecting the rejection of organic solutes during NF/RO treatment—a literature review. *Water Research, 38*(12), 2795-2809. doi:https://doi.org/10.1016/j.watres.2004.03.034

Bellona, C., Marts, M., & Drewes, J. E. (2010). The effect of organic membrane fouling on the properties and rejection characteristics of nanofiltration membranes. *Separation and Purification Technology, 74*(1), 44-54. doi:https://doi.org/10.1016/j.seppur.2010.05.006

Boonya-atichart, A., Boontanon, S. K., & Boontanon, N. (2016). Removal of perfluorooctanoic acid (PFOA) in groundwater by nanofiltration membrane. *Water Science and Technology, 74*(11), 2627-2633. doi:10.2166/wst.2016.434

Chaparro-Ortega, A., Betancourt, M., Rosas, P., Vázquez-Cuevas, F. G., Chavira, R., Bonilla, E., . . . Ducolomb, Y. (2018). Endocrine disruptor effect of perfluorooctane sulfonic acid (PFOS) and perfluorooctanoic acid (PFOA) on porcine ovarian cell steroidogenesis. *Toxicology in Vitro, 46*, 86-93. doi:https://doi.org/10.1016/j.tiv.2017.09.030

Childress, A. E., & Elimelech, M. (1996). Effect of solution chemistry on the surface charge of polymeric reverse osmosis and nanofiltration membranes. *Journal of Membrane Science, 119*(2), 253-268. doi:https://doi.org/10.1016/0376-7388(96)00127-5

Chon, K., KyongShon, H., & Cho, J. (2012). Membrane bioreactor and nanofiltration hybrid system for reclamation of municipal wastewater: Removal of nutrients, organic matter and micropollutants. *Bioresource Technology, 122*, 181-188. doi:https://doi.org/10.1016/j.biortech.2012.04.048

Dickenson, E. R. V., & Higgins, C. (2016). *Treatment Mitigation Strategies for Poly- and Perfluoroalkyl Substances* (Project #4322). Retrieved from Denver, Colorado: http://www.waterrf.org/PublicReportLibrary/4322.pdf

Du, Z., Deng, S., Chen, Y., Wang, B., Huang, J., Wang, Y., & Yu, G. (2015). Removal of perfluorinated carboxylates from washing wastewater of perfluorooctanesulfonyl fluoride using activated carbons and resins. *Journal of Hazardous Materials, 286*(Supplement C), 136-143. doi:https://doi.org/10.1016/j.jhazmat.2014.12.037

Flores, C., Ventura, F., Martin-Alonso, J., & Caixach, J. (2013). Occurrence of perfluorooctane sulfonate (PFOS) and perfluorooctanoate (PFOA) in N.E. Spanish surface waters and their removal in a drinking water treatment plant that combines conventional and advanced treatments in parallel lines. *Science of The Total Environment, 461-462*(Supplement C), 618-626. doi:https://doi.org/10.1016/j.scitotenv.2013.05.026

Hang, X., Chen, X., Luo, J., Cao, W., & Wan, Y. (2015). Removal and recovery of perfluorooctanoate from wastewater by nanofiltration. *Separation and Purification Technology, 145*(Supplement C), 120-129. doi:https://doi.org/10.1016/j.seppur.2015.03.013

John C. Crittenden, R. R. T., David W. Hand, Kerry J. Howe, George Tchobanoglous. (2012). *Water Treatment Principles and Design* (Third edition ed.). New Jersey: John Wiley & Sons, Inc.

Kim, H.-A., Choi, J.-H., & Takizawa, S. (2007). Comparison of initial filtration resistance by pretreatment processes in the nanofiltration for drinking water treatment. *Separation and Purification Technology, 56*(3), 354-362. doi:https://doi.org/10.1016/j.seppur.2007.02.016

Konwick, B. J., Tomy, G. T., Ismail, N., Peterson, J. T., Fauver, R. J., Higginbotham, D., & Fisk, A. T. (2008). Concentrations and patterns of perfluoroalkyl acids in Georgia, USA surface

waters near and distant to a major use source. *Environmental Toxicology and Chemistry, 27*(10), 2011-2018. doi:10.1897/07-659.1

Kothawala, D. N., Köhler, S. J., Östlund, A., Wiberg, K., & Ahrens, L. (2017). Influence of dissolved organic matter concentration and composition on the removal efficiency of perfluoroalkyl substances (PFASs) during drinking water treatment. *Water Research, 121*, 320-328. doi:https://doi.org/10.1016/j.watres.2017.05.047

Labban, O., Liu, C., Chong, T. H., & Lienhard V, J. H. (2017). Fundamentals of low-pressure nanofiltration: Membrane characterization, modeling, and understanding the multi-ionic interactions in water softening. *Journal of Membrane Science, 521*, 18-32. doi:https://doi.org/10.1016/j.memsci.2016.08.062

Lee, E., Shon, H. K., & Cho, J. (2010). Biofouling characteristics using flow field-flow fractionation: Effect of bacteria and membrane properties. *Bioresource Technology, 101*(5), 1487-1493. doi:https://doi.org/10.1016/j.biortech.2009.08.041

Mohammad, A. W., & Ali, N. a. (2002). Understanding the steric and charge contributions in NF membranes using increasing MWCO polyamide membranes. *Desalination, 147*(1), 205-212. doi:https://doi.org/10.1016/S0011-9164(02)00535-0

Moon, J., Lee, S., Song, J.-H., & Cho, J. (2010). Membrane fouling indicator of effluent organic matter with nanofiltration for wastewater reclamation, as obtained from flow field-flow fractionation. *Separation and Purification Technology, 73*(2), 164-172. doi:https://doi.org/10.1016/j.seppur.2010.03.020

Nicolini, J. V., Borges, C. P., & Ferraz, H. C. (2016). Selective rejection of ions and correlation with surface properties of nanofiltration membranes. *Separation and Purification Technology, 171*, 238-247. doi:https://doi.org/10.1016/j.seppur.2016.07.042

Oatley, D. L., Llenas, L., Pérez, R., Williams, P. M., Martínez-Lladó, X., & Rovira, M. (2012). Review of the dielectric properties of nanofiltration membranes and verification of the single oriented layer approximation. *Advances in Colloid and Interface Science, 173*, 1-11. doi:https://doi.org/10.1016/j.cis.2012.02.001

Ochoa-Herrera, V., & Sierra-Alvarez, R. (2008). Removal of perfluorinated surfactants by sorption onto granular activated carbon, zeolite and sludge. *Chemosphere, 72*(10), 1588-1593. doi:https://doi.org/10.1016/j.chemosphere.2008.04.029

Post, G. B., Cohn, P. D., & Cooper, K. R. (2012). Perfluorooctanoic acid (PFOA), an emerging drinking water contaminant: A critical review of recent literature. *Environmental Research, 116*, 93-117. doi:https://doi.org/10.1016/j.envres.2012.03.007

Post, G. B., Louis, J. B., Cooper, K. R., Boros-Russo, B. J., & Lippincott, R. L. (2009). Occurrence and Potential Significance of Perfluorooctanoic Acid (PFOA) Detected in New Jersey Public Drinking Water Systems. *Environmental Science & Technology, 43*(12), 4547-4554. doi:10.1021/es900301s

Pramanik, B. K., Pramanik, S. K., Sarker, D. C., & Suja, F. (2017). Removal of emerging perfluorooctanoic acid and perfluorooctane sulfonate contaminants from lake water. *Environmental Technology, 38*(15), 1937-1942. doi:10.1080/09593330.2016.1240716

Quiñones, O., & Snyder, S. A. (2009). Occurrence of Perfluoroalkyl Carboxylates and Sulfonates in Drinking Water Utilities and Related Waters from the United States. *Environmental Science & Technology, 43*(24), 9089-9095. doi:10.1021/es9024707

Rodea-Palomares, I., Leganés, F., Rosal, R., & Fernández-Piñas, F. (2012). Toxicological interactions of perfluorooctane sulfonic acid (PFOS) and perfluorooctanoic acid (PFOA) with selected pollutants. *Journal of Hazardous Materials, 201-202*, 209-218. doi:https://doi.org/10.1016/j.jhazmat.2011.11.061

Sadmani, A. H. M. A., Andrews, R. C., & Bagley, D. M. (2014). Rejection of pharmaceutically active and endocrine disrupting compounds by nanofiltration as a function of source water humic substances. *Journal of Water Process Engineering, 2*(Supplement C), 63-70. doi:https://doi.org/10.1016/j.jwpe.2014.05.004

Senevirathna, S. T. M. L. D., Tanaka, S., Fujii, S., Kunacheva, C., Harada, H., Shivakoti, B. R., & Okamoto, R. (2010). A comparative study of adsorption of perfluorooctane sulfonate (PFOS) onto granular activated carbon, ion-exchange polymers and non-ion-exchange polymers. *Chemosphere, 80*(6), 647-651. doi:https://doi.org/10.1016/j.chemosphere.2010.04.053

Shoemaker, J., Grimmett, P., & Boutin, B. (2009). Determination of selected perfluorinated alkyl acids in drinking water by solid-phase extraction and liquid chromatography/tandem mass spectrometry (LC/MS/MS). *Tandem Mass Spectrometry (LC/MS/MS), in, US Environmental Protection Agency, Washington, DC*.

Soriano, Á., Gorri, D., & Urtiaga, A. (2017). Efficient treatment of perfluorohexanoic acid by nanofiltration followed by electrochemical degradation of the NF concentrate. *Water Research, 112*(Supplement C), 147-156. doi:https://doi.org/10.1016/j.watres.2017.01.043

Standard Methods for the Examination of Water and Wastewater. (2012). *American Public Health Association*.

Steinle-Darling, E., & Reinhard, M. (2008). *Nanofiltration for Trace Organic Contaminant Removal: Structure, Solution, and Membrane Fouling Effects on the Rejection of Perfluorochemicals* (Vol. 42).

Stigaard Kjeldsen, L., & Bonefeld-Jørgensen, E. C. (2013). *Perfluorinated compounds affect the function of sex hormone receptors* (Vol. 20).

Suja, F., Pramanik, B., & Md Zain, S. (2009). *Contamination, bioaccumulation and toxic effects of perfluorinated chemicals (PFCs) in the water environment: A review paper* (Vol. 60).

Tang, C. Y., Fu, Q. S., Criddle, C. S., & Leckie, J. O. (2007). Effect of Flux (Transmembrane Pressure) and Membrane Properties on Fouling and Rejection of Reverse Osmosis and Nanofiltration Membranes Treating Perfluorooctane Sulfonate Containing Wastewater. *Environmental Science & Technology, 41*(6), 2008-2014. doi:10.1021/es062052f

Thompson, J., Eaglesham, G., Reungoat, J., Poussade, Y., Bartkow, M., Lawrence, M., & Mueller, J. F. (2011). Removal of PFOS, PFOA and other perfluoroalkyl acids at water reclamation plants in South East Queensland Australia. *Chemosphere, 82*(1), 9-17. doi:https://doi.org/10.1016/j.chemosphere.2010.10.040

USEPA. (2016, November 2016). PFOA and PFOs Drinking Water Health Advisories. Retrieved from https://www.epa.gov/sites/production/files/2016-06/documents/drinkingwaterhealthadvisories_pfoa_pfos_updated_5.31.16.pdf

Wang, F., & Shih, K. (2011). Adsorption of perfluorooctanesulfonate (PFOS) and perfluorooctanoate (PFOA) on alumina: Influence of solution pH and cations. *Water Research, 45*(9), 2925-2930. doi:https://doi.org/10.1016/j.watres.2011.03.007

Wang, J., Wang, L., Xu, C., Zhi, R., Miao, R., Liang, T., . . . Liu, T. (2018). Perfluorooctane sulfonate and perfluorobutane sulfonate removal from water by nanofiltration membrane: The roles of solute concentration, ionic strength, and macromolecular organic foulants. *Chemical Engineering Journal, 332*, 787-797. doi:https://doi.org/10.1016/j.cej.2017.09.061

Wang, T., Zhao, C., Li, P., Li, Y., & Wang, J. (2015). Fabrication of novel poly(m-phenylene isophthalamide) hollow fiber nanofiltration membrane for effective removal of trace amount perfluorooctane sulfonate from water. *Journal of Membrane Science, 477*, 74-85. doi:https://doi.org/10.1016/j.memsci.2014.12.038

Wilf, M. (2007). *The Guidebook to Membrane Desalination Technology*. Hopkinton, MA 01748, USA: Desalinations Publications.

Xiao, F., Simcik, M., & Gulliver, J. (2012). *Mechanisms for removal of perfluorooctane sulfonate (PFOS) and perfluorooctanoate (PFOA) from drinking water by conventional and enhanced coagulation* (Vol. 47).

Xiao, F., Simcik, M. F., & Gulliver, J. S. (2013). Mechanisms for removal of perfluorooctane sulfonate (PFOS) and perfluorooctanoate (PFOA) from drinking water by conventional and enhanced coagulation. *Water Research, 47*(1), 49-56. doi:https://doi.org/10.1016/j.watres.2012.09.024

Xiao, F., Simcik, M. F., Halbach, T. R., & Gulliver, J. S. (2015). Perfluorooctane sulfonate (PFOS) and perfluorooctanoate (PFOA) in soils and groundwater of a U.S. metropolitan area: Migration and implications for human exposure. *Water Research, 72*(Supplement C), 64-74. doi:https://doi.org/10.1016/j.watres.2014.09.052

Xu, M., Cui, Z., Zhao, L., Hu, S., Zong, W., & Liu, R. (2018). Characterizing the binding interactions of PFOA and PFOS with catalase at the molecular level. *Chemosphere, 203*, 360-367. doi:https://doi.org/10.1016/j.chemosphere.2018.03.200

Yangali-Quintanilla, V., Sadmani, A., McConville, M., Kennedy, M., & Amy, G. (2009). Rejection of pharmaceutically active compounds and endocrine disrupting compounds by clean and fouled nanofiltration membranes. *Water Research, 43*(9), 2349-2362. doi:https://doi.org/10.1016/j.watres.2009.02.027

Yu, Q., Zhang, R., Deng, S., Huang, J., & Yu, G. (2009). Sorption of perfluorooctane sulfonate and perfluorooctanoate on activated carbons and resin: Kinetic and isotherm study. *Water Research, 43*(4), 1150-1158. doi:https://doi.org/10.1016/j.watres.2008.12.001

Yu, Y., Zhao, C., Yu, L., Li, P., Wang, T., & Xu, Y. (2016). Removal of perfluorooctane sulfonates from water by a hybrid coagulation–nanofiltration process. *Chemical Engineering Journal, 289*, 7-16. doi:https://doi.org/10.1016/j.cej.2015.12.048

Zaggia, A., Conte, L., Falletti, L., Fant, M., & Chiorboli, A. (2016). Use of strong anion exchange resins for the removal of perfluoroalkylated substances from contaminated drinking water in batch and continuous pilot plants. *Water Research, 91*(Supplement C), 137-146. doi:https://doi.org/10.1016/j.watres.2015.12.039

Zhang, L., Niu, J., Wang, Y., Shi, J., & Huang, Q. (2014). Chronic effects of PFOA and PFOS on sexual reproduction of freshwater rotifer Brachionus calyciflorus. *Chemosphere, 114*, 114-120. doi:https://doi.org/10.1016/j.chemosphere.2014.03.099

Zhao, C., Hu, G., Hou, D., Yu, L., Zhao, Y., Wang, J., . . . Zhai, Y. (2018). Study on the effects of cations and anions on the removal of perfluorooctane sulphonate by nanofiltration membrane. *Separation and Purification Technology, 202*, 385-396. doi:https://doi.org/10.1016/j.seppur.2018.03.046

Zhao, C., Tang, C. Y., Li, P., Adrian, P., & Hu, G. (2016). Perfluorooctane sulfonate removal by nanofiltration membrane—the effect and interaction of magnesium ion / humic acid. *Journal of Membrane Science, 503*, 31-41. doi:https://doi.org/10.1016/j.memsci.2015.12.049

Zhao, C., Zhang, J., He, G., Wang, T., Hou, D., & Luan, Z. (2013). Perfluorooctane sulfonate removal by nanofiltration membrane the role of calcium ions. *Chemical Engineering Journal, 233*, 224-232. doi:https://doi.org/10.1016/j.cej.2013.08.027